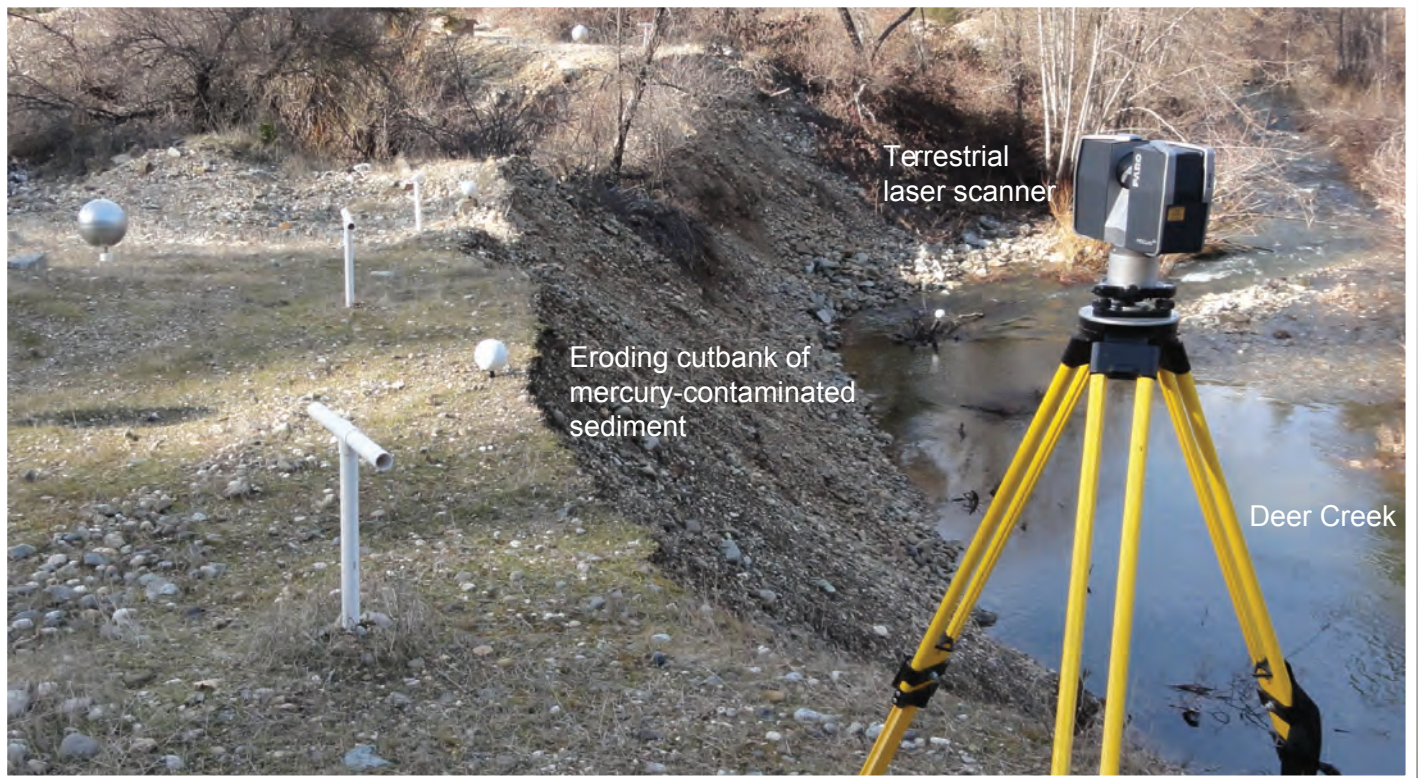


Prepared in cooperation with the Bureau of Land Management

Quantifying the Eroded Volume of Mercury-Contaminated Sediment Using Terrestrial Laser Scanning at Stocking Flat, Deer Creek, Nevada County, California, 2010–13



Scientific Investigations Report 2015–5179

Cover.

Front image—A FARO Focus³⁰ laser scanner on top of eroding cutbank at Stocking Flat study site, February 4, 2013.

Back top image—Oblique image for a selected 4-meter-wide area of the cutbank showing retreat of the cutbank surface between January 2011 and February 2013. The oblique perspective is looking downstream and the selected area is the foreground of the cutbank shown in the cover photo, just beyond the tripod and laser scanner.

Back bottom image—Color-coded difference plot showing the horizontal change, in meters, from January 2011 to February 2013 for the selected area shown in the above image.

Quantifying the Eroded Volume of Mercury-Contaminated Sediment Using Terrestrial Laser Scanning at Stocking Flat, Deer Creek, Nevada County, California, 2010–13

By James F. Howle, Charles N. Alpers, Gerald W. Bawden, and Sandra Bond

Prepared in cooperation with the Bureau of Land Management

Scientific Investigations Report 2015–5179

U.S. Department of the Interior
U.S. Geological Survey

U.S. Department of the Interior
SALLY JEWELL, Secretary

U.S. Geological Survey
Suzette M. Kimball, Director

U.S. Geological Survey, Reston, Virginia: 2016

For more information on the USGS—the Federal source for science about the Earth, its natural and living resources, natural hazards, and the environment—visit <http://www.usgs.gov> or call 1–888–ASK–USGS.

For an overview of USGS information products, including maps, imagery, and publications, visit <http://store.usgs.gov/>.

Any use of trade, firm, or product names is for descriptive purposes only and does not imply endorsement by the U.S. Government.

Although this information product, for the most part, is in the public domain, it also may contain copyrighted materials as noted in the text. Permission to reproduce copyrighted items must be secured from the copyright owner.

Suggested citation:

Howle, J.F., Alpers, C.N., Bawden, G.W., and Bond, Sandra, 2016, Quantifying the eroded volume of mercury-contaminated sediment using terrestrial laser scanning at Stocking Flat, Deer Creek, Nevada County, California, 2010–13: U.S. Geological Survey Scientific Investigations Report 2015–5179, 23 p., <http://dx.doi.org/10.3133/SIR20155179>.

ISSN 2328-0328 (online)

Contents

| | |
|--------------------------------------|----|
| Abstract | 1 |
| Introduction..... | 1 |
| Purpose and Scope | 3 |
| Study Area Description..... | 3 |
| Methods..... | 3 |
| Data Collection..... | 4 |
| Point-Cloud Alignment | 5 |
| Geometric Benchmarks..... | 5 |
| Reference Points | 5 |
| Alignment of Sequential Surveys..... | 7 |
| Quality Assurance of Alignments..... | 8 |
| Volumetric Determination..... | 8 |
| Data-Point Removal..... | 8 |
| Creating Surfaces..... | 8 |
| Defining a Common Boundary..... | 9 |
| Calculating Volumetric Changes..... | 9 |
| Results of Volume Calculations | 10 |
| Visualization of Changes..... | 14 |
| Shaded-Relief Images..... | 14 |
| Two-Dimensional Change Maps | 16 |
| Three-Dimensional Anaglyphs | 20 |
| Summary..... | 20 |
| References Cited..... | 21 |
| Glossary..... | 23 |

Figures

| | |
|--|----|
| 1. Maps and photographs showing location of Deer Creek in the Yuba River drainage basin of northern California | 2 |
| 2. Photographs showing an Optech ILRIS 36D laser scanner deployed in two locations at Stocking Flat, Deer Creek, Nevada County, California..... | 4 |
| 3. Graphics output from PolyWorks® software package showing an example of alignment and comparison of overlapping point-cloud data | 6 |
| 4. Photograph showing a FARO Focus ^{3D} laser scanner on top of eroding cutbank at Stocking Flat study site, February 4, 2013 | 6 |
| 5. Images showing sequence for defining reference points from geometric benchmarks | 7 |
| 6. Graphics output from PolyWorks® software showing the sequence for calculating volume | 10 |
| 7. Graphics output from PolyWorks® software showing lidar point cloud of the cutbank surface..... | 13 |
| 8. Images showing shaded-relief oblique views of Stocking Flat cutbank study site near Nevada City, California, for the four surveys between December 2010 and February 2013 | 15 |

Figures—Continued

9. Photograph showing the central part of the cutbank on March 17, 2011, high streamflow and the near-vertical fluvial scarp.....16
10. Graphics output from PolyWorks® software showing difference maps of horizontal change across the cutbank surface for four periods between December 1, 2010, and February 4, 201317
11. Images showing three-dimensional anaglyphs and two-dimensional difference maps showing changes from December 2010 to February 2013 for selected areas of the cutbank.....18
12. Images showing three-dimensional anaglyph and two-dimensional difference maps showing changes from January 2011 to February 2013 for a selected area of the cutbank19

Tables

1. Calculated volumes between the cutbank surface and reference planes for surveys 1, 2, 3, and 4.....11
2. Measured volumes of mercury-contaminated sediment (in cubic meters) eroded from the Stocking Flat cutbank study site for various periods between December 1, 2010, and February 4, 2013.....14

Conversion Factors

International System of Units to Inch/Pound

| Multiply | By | To obtain |
|--------------------------------------|---------|--------------------------------|
| Length | | |
| centimeter (cm) | 0.3937 | inch (in.) |
| millimeter (mm) | 0.03937 | inch (in.) |
| meter (m) | 3.281 | foot (ft) |
| kilometer (km) | 0.6214 | mile (mi) |
| meter (m) | 1.094 | yard (yd) |
| Area | | |
| square meter (m ²) | 10.76 | square foot (ft ²) |
| square centimeter (cm ²) | 0.1550 | square inch (in ²) |
| Volume | | |
| cubic meter (m ³) | 35.31 | cubic foot (ft ³) |
| Mass | | |
| kilogram (kg) | 2.205 | pound avoirdupois (lb) |

Temperature in degrees Celsius (°C) may be converted to degrees Fahrenheit (°F) as
 $^{\circ}\text{F} = (1.8 \times ^{\circ}\text{C}) + 32$.

Temperature in degrees Fahrenheit (°F) may be converted to degrees Celsius (°C) as
 $^{\circ}\text{C} = (^{\circ}\text{F} - 32) / 1.8$.

Abbreviations and Acronyms

| | |
|-------|--|
| 2-D | two dimensional |
| 3-D | three dimensional |
| ASL | above sea level |
| BLM | Bureau of Land Management |
| Hg | mercury |
| lidar | light detection and ranging (or LiDAR) |
| PVC | polyvinyl chloride |
| RMSE | root-mean-square error |
| TIN | triangulated irregular network |
| TLS | terrestrial laser scanning |
| USGS | United States Geological Survey |
| VR | virtual reality |
| Vrui | Virtual reality user interface |
| WY | water year |

Selected technical terms are defined in the glossary. These terms are indicated in bold font the first time they are used in the main body of the report.

Quantifying the Eroded Volume of Mercury-Contaminated Sediment Using Terrestrial Laser Scanning at Stocking Flat, Deer Creek, Nevada County, California, 2010–13

By James F. Howle, Charles N. Alpers, Gerald W. Bawden, and Sandra Bond

Abstract

High-resolution ground-based light detection and ranging (lidar), also known as terrestrial laser scanning, was used to quantify the volume of mercury-contaminated sediment eroded from a stream cutbank at Stocking Flat along Deer Creek in the Sierra Nevada foothills, about 3 kilometers west of Nevada City, California. Terrestrial laser scanning was used to collect sub-centimeter, three-dimensional images of the complex cutbank surface, which could not be mapped non-destructively or in sufficient detail with traditional surveying techniques.

The stream cutbank, which is approximately 50 meters long and 8 meters high, was surveyed on four occasions: December 1, 2010; January 20, 2011; May 12, 2011; and February 4, 2013. Volumetric changes were determined between the sequential, three-dimensional lidar surveys. Volume was calculated by two methods, and the average value is reported. Between the first and second surveys (December 1, 2010, to January 20, 2011), a volume of 143 plus or minus 15 cubic meters of sediment was eroded from the cutbank and mobilized by Deer Creek. Between the second and third surveys (January 20, 2011, to May 12, 2011), a volume of 207 plus or minus 24 cubic meters of sediment was eroded from the cutbank and mobilized by the stream. Total volumetric change during the winter and spring of 2010–11 was 350 plus or minus 28 cubic meters. Between the third and fourth surveys (May 12, 2011, to February 4, 2013), the differencing of the three-dimensional lidar data indicated that a volume of 18 plus or minus 10 cubic meters of sediment was eroded from the cutbank. The total volume of sediment eroded from the cutbank between the first and fourth surveys was 368 plus or minus 30 cubic meters.

Introduction

On the western slope of the Sierra Nevada, historical **hard-rock** (lode) and **placer** (gravel) mines produced large volumes of mercury (Hg)-contaminated **mining debris**

(Gilbert, 1917; James, 1989). Elemental Hg was used extensively to enhance gold recovery during the mid-to-late 1800s and the early 1900s (Alpers and others, 2005a), which resulted in Hg contamination of sediment in many areas throughout the Sierra Nevada, including the Yuba River drainage basin, Deer Creek subbasin, and the Stocking Flat study site (fig. 1). Although Hg was used both in hard-rock and in placer gold-mining operations, historical records indicated that much more Hg was used and lost to the environment from placer gold-mining activities in the Sierra Nevada than from hard-rock mines and associated mills (Churchill, 2000; Alpers and others, 2005a).

To identify Hg “hot spots” for remediation targets in the Deer Creek drainage basin and other areas in the Sierra Nevada, the U.S. Geological Survey (USGS) has been working in cooperation with the Bureau of Land Management (BLM) and other federal, state, and local agencies on regional and detailed studies since 1999 (Hunerlach and others, 1999, 2004; May and others, 2000; Alpers and others, 2005a, 2005b, 2006, 2012; Fleck and others, 2011; Marvin-DiPasquale and others, 2011). In the Deer Creek drainage basin, methylmercury concentrations in water, sediment, fish (primarily brown trout and largemouth bass), and predatory invertebrates (larval dragonflies, mayflies, stoneflies, and adult water striders) were monitored during 2010 and 2011 to assess temporal and spatial variability in stream environments upstream and downstream from suspected mercury sources (Jacob Fleck and others, U.S. Geological Survey, written commun., 2015).

The Stocking Flat study site lies along Deer Creek about 3 kilometers (km) west of Nevada City, California (figs. 1B, C). Several large historical hard-rock gold mines (Champion, Providence, and Mountaineer) and associated mills are less than 2.5 km upstream from Stocking Flat. In addition to these hard-rock mines, there were small-to-medium sized **hydraulic gold mines** in the areas that are now Hirschman’s Pond and Scotts Flat Reservoir (fig. 1B). During the late 19th and early 20th centuries, the Deer Creek drainage at Stocking Flat became filled with sediment consisting largely of mining debris from upstream hard-rock and placer mines (fig. 1C).

2 Quantifying Mercury-Contaminated Sediment at Stocking Flat, Deer Creek, Nevada County, Calif., 2010–13

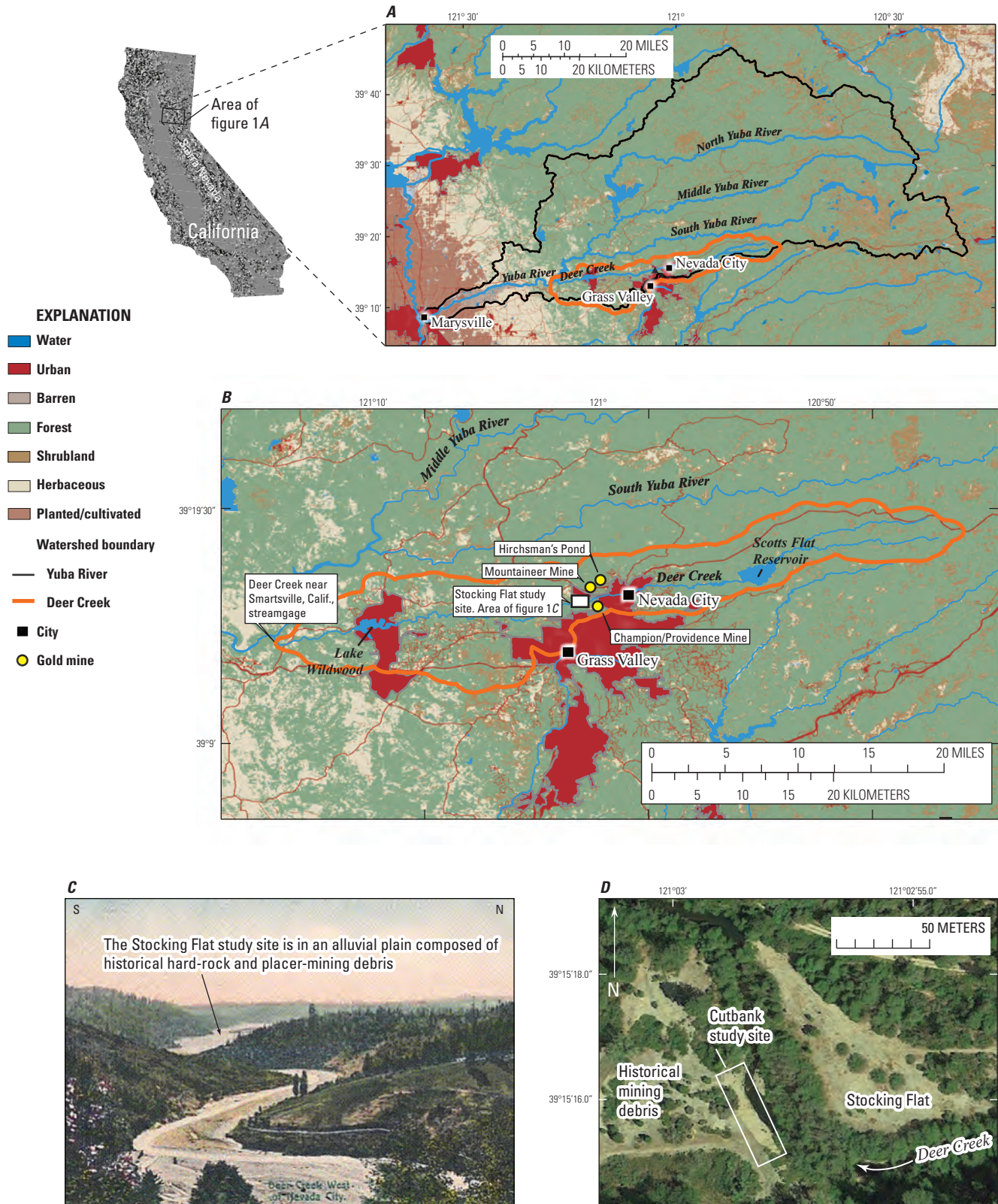


Figure 1. A, Location of Deer Creek in the Yuba River drainage basin of northern California; B, the Deer Creek drainage basin showing geographic locations discussed in text; C, undated historical photo showing the Deer Creek drainage looking west, downstream from Nevada City; and D, aerial photograph of Stocking Flat, with an arrow showing the direction of streamflow in Deer Creek.

Deer Creek, a major tributary to the Yuba River (fig. 1A), has incised into these contaminated sediments for many years, thus increasing the potential for mobilization of Hg to downstream areas.

Terrestrial laser scanning (TLS) is a remote-sensing technology that can collect high-resolution (sub-centimeter), three-dimensional (3-D) measurements of the land surface that cannot be achieved with traditional surveying techniques (Heritage and Large, 2009). Sometimes TLS is referred to as terrestrial **lidar** or tripod-mounted lidar (T-lidar). A laser scanner or lidar scanner emits pulses of near-infrared laser light that are timed to measure the distance (range) from the laser scanner to the reflecting surface. Laser ranges are combined with angular orientation data to generate a dense and detailed set of x, y, and z points (locations of individual laser returns) referred to as a **point cloud**. The non-destructive sampling of the unconsolidated cutbank sediments and the sub-centimeter precision of the point cloud allows for a spatially detailed assessment of change across the cutbank surface.

In this study, four sequential TLS surveys of the stream cutbank were completed. Each survey period was composed of multiple TLS scans collected from different vantages that were combined into a composite 3-D point cloud of the stream cutbank. The sequential surveys were co-registered, or ‘aligned,’ into a common 3-D reference frame so that volumetric comparisons between the surveys could be made. The difference in volume between sequential surveys is the amount of sediment removed from the cutbank by erosion and mobilized by the stream. Volume was calculated by two methods, and the average value was reported.

Purpose and Scope

The purpose of this report is (1) to document the methods used to quantify the volume of Hg-contaminated sediment eroded from a discrete section of stream cutbank along Deer Creek at Stocking Flat (fig. 1D), an area managed by the BLM, and (2) to quantify the volume of eroded sediment (incremental and total) for three periods between December 1, 2010, and February 4, 2013.

The results of this study have been combined with laboratory determinations of Hg concentration and grain-size distribution (Jacob Fleck and others, U.S. Geological Survey, written commun., 2015) to quantify the amount of Hg eroded into Deer Creek downstream from the cutbank. Results from these investigations are to be used by the BLM to determine whether removal or stabilization of Hg-contaminated sediment is needed at the Stocking Flat study site.

The TLS approach also provides information regarding the physical processes of cutbank erosion, such as stream under-cutting and slumping. This information could be useful to the BLM for stabilizing Hg-contaminated sediment at Stocking Flat and similar sites elsewhere. A suite of innovative

visualization graphics, including 3-D images, is included in this report to facilitate understanding of the physical processes.

Study Area Description

The Stocking Flat study site is along Deer Creek in the foothills of the Sierra Nevada (fig. 1), where the topographic relief is approximately 200 meters (m) from the valley floor to surrounding ridge lines. The cutbank-study site at Stocking Flat is at an elevation of 650 m above sea level (ASL) and is on an alluvial plain largely composed of mining debris fluviually transported from upstream historical hard-rock and placer gold mines (fig. 1C). The Deer Creek drainage basin, a major tributary in the Yuba River drainage basin (fig. 1A), ranges in elevation from approximately 90 m ASL at the confluence with the main stem of the Yuba River to more than 1,500-m ASL at the headwaters. The stream cutbank at Stocking Flat is approximately 50 m long and 8 m high and covers about 400 square meters (m²).

The climate in the study area is Mediterranean, with warm-to-hot, dry summers and cool, rainy winters. The long-term precipitation gage nearest to the Stocking Flat study site is approximately 4.5 km to the south-southwest, at Grass Valley, California (fig. 1). The average annual **water-year (WY)** precipitation at Grass Valley, California, is 1.34 m (or 52.80 inches, in.). For WY 2011 (October 2010 through September 2011), the total precipitation of 1.85 m (72.81 in.) was 138 percent of the long-term average, and the WY 2012 total of 1.19 m (46.74 in.) was 88 percent of the long-term average. Similarly, total precipitation in WY 2013 of 1.20 m (47.21 in.) was 89 percent of the long-term average. Daily precipitation data for this gage for WY 1967 through 2013 are available at <http://www.ncdc.noaa.gov/cdo-web/search> (National Weather Service Station GHCND: USC00043573, GRASS VALLEY NUMBER 2, CA US, last accessed August 28, 2014).

The closest USGS streamgage (11418500) is at the lower end of the Deer Creek drainage near Smartsville, California, approximately 20 km west-southwest (downstream) of the Stocking Flat study site (fig. 1B). It was not feasible to use the data from this streamgage to estimate stream discharge at the Stocking Flat study site because a reservoir (Lake Wildwood) between Stocking Flat and the streamgage (fig. 1B) retained storm-water runoff during periods of heavy precipitation.

Methods

This section contains information on methods of TLS data collection, point-cloud alignment, and volumetric calculations. Information on quality assurance is included to explain how uncertainties in volume calculations were quantified.

Data Collection

The cutbank and the terrace above it were surveyed on four occasions: December 1, 2010; January 20, 2011; May 12, 2011; and February 4, 2013. These surveys were used to determine the volume of sediment eroded between the surveys by assessing the 3-D difference in the cutbank surfaces from one survey to another.

Data from the first three TLS surveys (during 2010 and 2011) were collected with an Optech ILRIS-36D laser scanner (Optech Inc., West Henrietta, New York; [fig. 2](#)). The laser returns from the Optech scanner have an x-y-z positional accuracy of plus or minus 4 millimeters (mm) at a distance of 100 m (according to manufacturer specifications). The target area for this study was less than 50 m from the scanner. The laser scanner, mounted on a rotating base ([fig. 2A](#)), panned the target area and collected a composite color image that

was displayed on a tablet personal computer (PC). On the tablet PC, the area to be scanned was defined, and the laser spot spacing was set to 7–9 mm, which yielded an average data density of more than 15,000 points for each square meter across the cutbank. Detailed inset areas of geometric bench marks, described later in this section, were defined to increase the data density of those targets to a laser spot spacing of 4 to 5 mm. During each survey, the laser scanner was deployed in two locations so the entire cutbank surface and the geometric benchmarks could be imaged by the laser scanner: (1) on the right bank of the stream across from the cutbank ([fig. 2A](#)) and (2) on the terrace above the cutbank ([fig. 2B](#)).

When the Optech scanner was used with the pan-and-tilt base ([fig. 2A](#)), the scanner systematically scanned the target area with a series of overlapping 40-degree by 40-degree scans. Each 40-degree-wide scan was collected with 8-degree (or 20-percent) overlap with the adjoining scan to ensure that the scans could be accurately aligned or combined into a composite point cloud by using the PolyWorks® software package (Version 12.0.15, InnovMetric Software Inc., Quebec City, Quebec, Canada). [Figure 3A](#) shows overlapping scans of the upstream part of the cutbank. The first light detection and ranging (lidar) scan (on left side of [fig. 3A](#)) is slightly in front of the second scan (on right side of [fig. 3A](#)). The sharp color change marks the downstream limit of the first scan. The two scans are slightly misaligned because the laser scanner was in a slightly different position for the second scan. This misalignment was corrected with an iterative algorithm that computed an optimal alignment by minimizing the distance between the overlapping 3-D point clouds. Through a series of rotations and translations, the overlapping point clouds were adjusted until a user-defined convergence, (here, 10^{-7} or less), between the two scans was achieved. A lesser convergence value represents a better 3-D alignment. The alignment is visually evident by the melding of the different color point clouds in the area of overlap ([fig. 3B](#)). The two-standard-deviation error (or 95-percent confidence interval) of the iterative alignments was typically on the order of 4–6 mm. In [figure 3C](#), the darkest color in the area of overlap indicates that the separation of the two aligned point clouds was less than 5 mm.

The fourth survey (February 4, 2013) was collected with a FARO Focus^{3D} laser scanner, which had less scatter in the point-cloud data than in previous surveys, leading to improved 3-D definition of the cutbank surface. Laser returns from the FARO scanner have positional accuracy of plus or minus 0.5 mm at a distance of 25 m (according to manufacturer specifications). Inspection of the FARO data in a fully immersive 3-D environment (Kellogg and others, 2008; Kreylos and others, 2008) showed that the positional accuracies across the cutbank surface were improved by using the FARO scanner compared to the point-cloud data collected with the Optech scanner for the first three surveys.

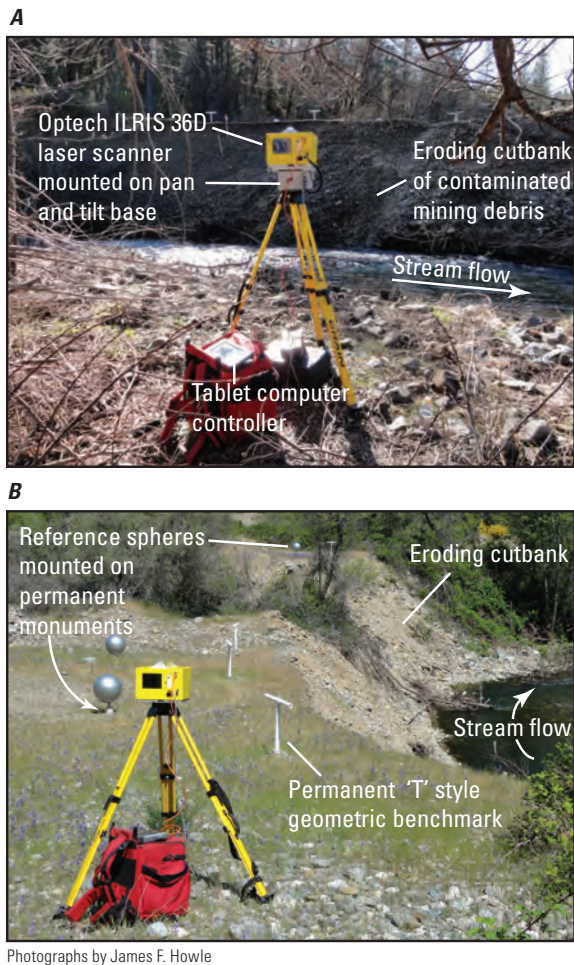


Figure 2. An Optech ILRIS 36D laser scanner deployed in two locations at Stocking Flat, Deer Creek, Nevada County, California: *A*, laser scanner mounted on pan-and-tilt base with cutbank in the background, view to the southwest, and *B*, laser scanner without pan-and-tilt base on top of cutbank terrace, with view to the north-northwest.

The improved positional accuracy of the FARO laser returns was achieved by averaging six laser pulses to determine each recorded point compared to the single pulse used by the Optech scanner. The FARO scanner, mounted on a standard survey tripod (fig. 4), rotated about the vertical axis, collecting a full 360-degree point cloud, except for a 60-degree-wide cone directly beneath the scanner. A pre-set laser spot spacing of 6.7 mm at a distance 10 m from the scanner origin was used. The cutbank and terrace areas were scanned from four different vantages (two setups from the right bank of the creek, facing the cutbank, and two setups on the left-bank terrace, above the cutbank). The combined data density from the four scans was more than 11,400 points per square meter, which is equivalent to a laser-spot spacing of approximately 9 mm.

The alignment of the four scans in the fourth (February 4, 2013) survey was accomplished with the software package SCENE (Version 4.0, FARO Technologies, Lake Mary, Florida). For each scan, the SCENE software automatically identified the 0.2-m-diameter reference spheres (fig. 4) and determined the relative positions of these spheres. The SCENE software then locked the position of the scan that had the greatest number of reference spheres, while the remaining scans were rotated and translated until the reference spheres were best fit in 3-D space relative to the locked scan. For the purpose of assessing the quality of the alignment, the SCENE software also calculated a root-mean-square error (RMSE, or one standard deviation) of the alignment. This error was computed from the spatial variations of the reference sphere center points for each unlocked scan relative to the locked scan. The 95-percent confidence interval of the alignment (two-standard-deviation error) was plus or minus 4.4 mm for the fourth survey.

Point-Cloud Alignment

To make comparisons between the different surveys, there must be stable and common benchmarks in each survey. For this study, two types of geometric benchmarks were used to register the surveys. The first benchmark type was a stable monument to which a removable reference sphere was attached, and the second benchmark type was a 'T' form constructed from polyvinyl chloride (PVC) pipe (fig. 5A). The following section describes the construction of the two types of geometric benchmarks that were installed on the terrace above the cutbank (fig. 5A).

Geometric Benchmarks

Three reference-sphere benchmarks were constructed by digging holes, approximately 0.3 m wide and 0.5 m deep, into the alluvium. Then, 1.2-m-long, 16-mm-diameter sections of threaded steel rod were driven into the alluvium at the center of the holes until 0.2 m of rod was left exposed above the ground surface. Each hole was backfilled to the land surface with about 30 kilograms (kg) of concrete. Approximately 0.15 m of the protruding rod was cased with 0.1-m-diameter PVC pipe and filled with concrete, leaving about 0.05 m (5 centimeters, cm) of threaded rod exposed (fig. 5A). Commercially available plastic spheres (0.45-m diameter) were fitted with threaded couplings. Each sphere was screwed onto a stable monument until the coupling bottomed out against the threaded rod of the monument. Linear reference marks on the sphere, coupling, and PVC casing were aligned so that each sphere could be repositioned on the corresponding monument to within plus or minus 4 mm.

Four reference 'T' benchmarks were constructed from readily available PVC pipe (with an outer diameter of 60 mm) and a PVC 'T' coupling. The constructed PVC 'T' benchmarks measured approximately 0.6 m wide by 1.0 m high. To anchor each 'T,' a hole approximately 0.3 m wide and 0.3 m deep was dug into the alluvium and anchored with about 20 kg of concrete.

Reference Points

After the scans for a given period were combined into a composite 3-D point cloud, reference points were defined from the point clouds of the geometric benchmarks by using the PolyWorks® software package. The spherical point clouds (more than 10.9×10^3 points per sphere, fig. 5B) were isolated in a 3-D environment and modeled as perfect spheres of a known radius (fig. 5C). From these "best-fit" spheres, the center points were mathematically derived as unique (x, y, z) points in 3-D space at millimeter resolution (fig. 5D). The repeatability of defining these points for any given sphere was plus or minus 0.4 mm (maximum variance along x, y, or z axis).

By using the point clouds of the PVC 'T's, reference points were defined at the intersection of perpendicular cylinder axes. In a 3-D visualization environment, the lidar point clouds of the PVC pipes (more than 6.5×10^3 points per 'T' excluding points on the 'T' couplings) were isolated and modeled as "best-fit" cylinders of a known radius (fig. 5C). The intersection of the perpendicular cylinder axes define (x, y, z) points in space at millimeter resolution (fig. 5D). The repeatability of defining these points in 3-D space was plus or minus 0.7 mm (maximum variance along an x, y, or z axis).

6 Quantifying Mercury-Contaminated Sediment at Stocking Flat, Deer Creek, Nevada County, Calif., 2010–13

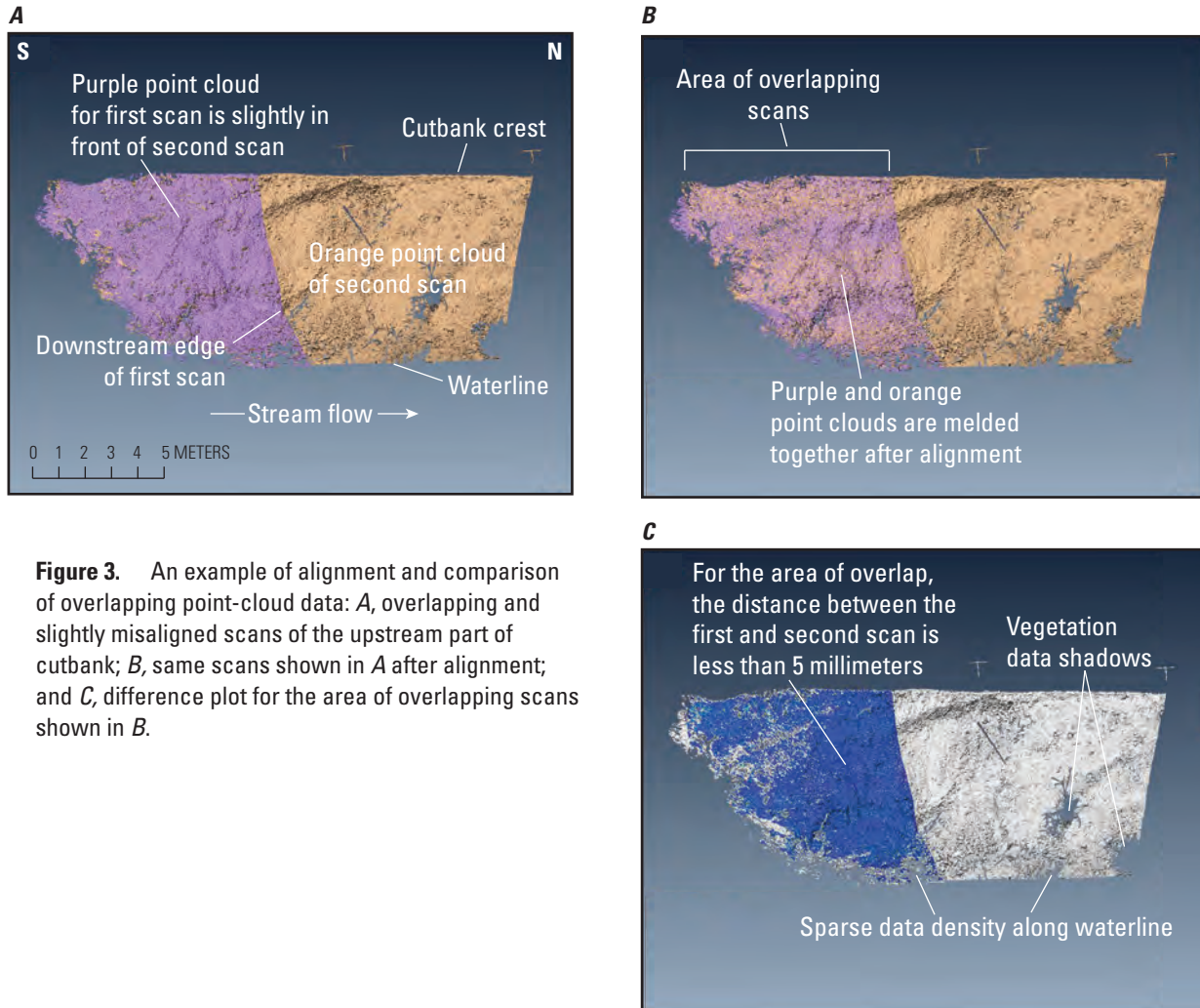
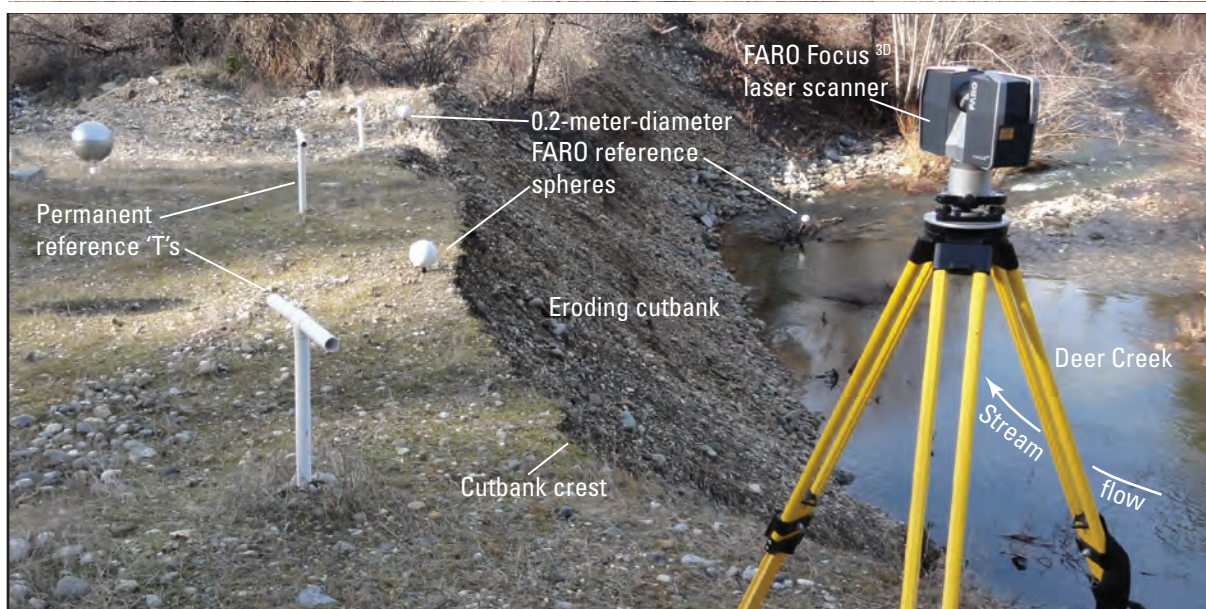
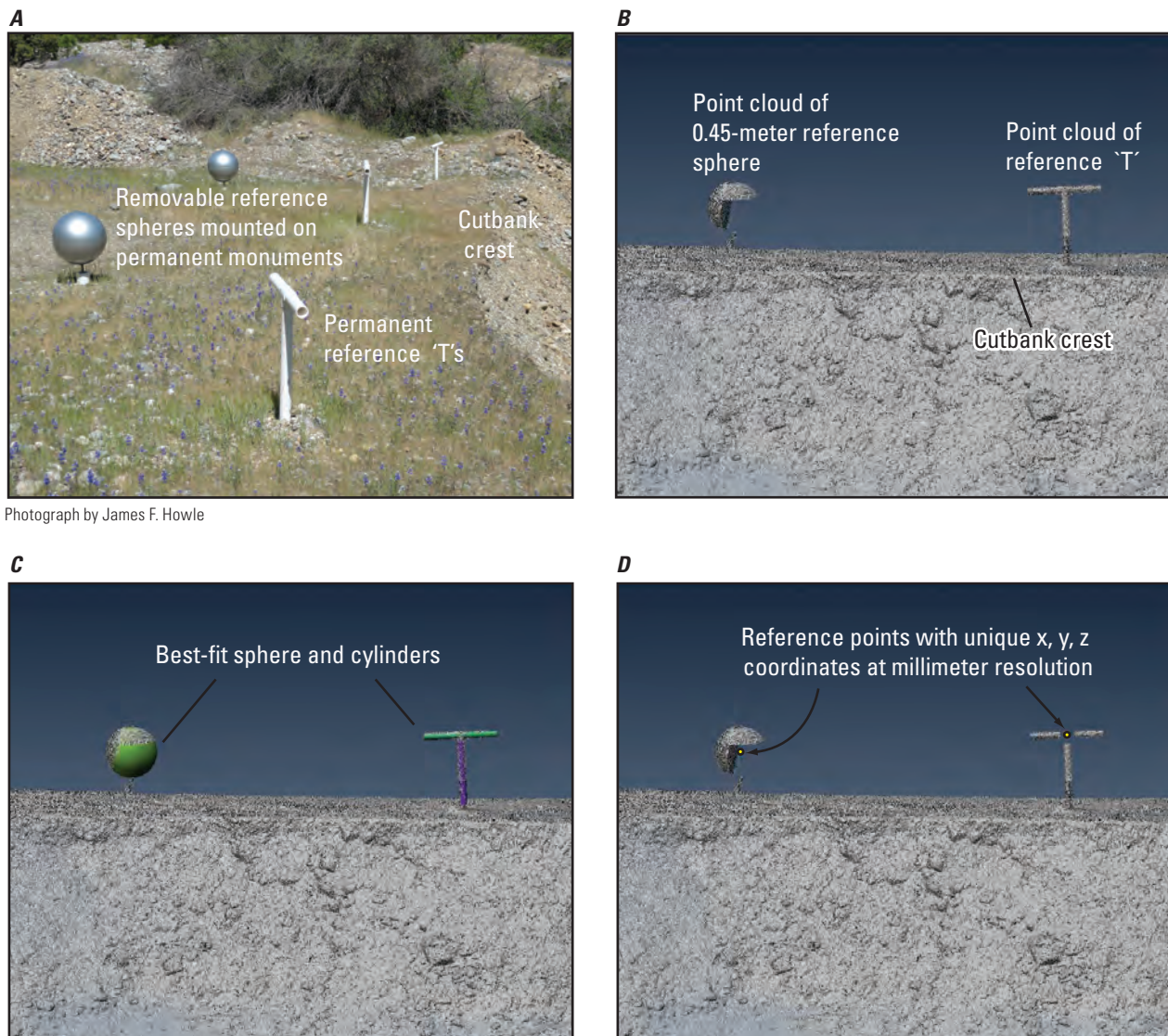


Figure 3. An example of alignment and comparison of overlapping point-cloud data: *A*, overlapping and slightly misaligned scans of the upstream part of cutbank; *B*, same scans shown in *A* after alignment; and *C*, difference plot for the area of overlapping scans shown in *B*.



Photograph by James F. Howle

Figure 4. A FARO Focus^{3D} laser scanner on top of eroding cutbank at Stocking Flat study site, February 4, 2013.



Photograph by James F. Howle

Figure 5. Sequence for defining reference points from geometric benchmarks. *A*, Photograph of removable reference spheres and semi-permanent reference 'T's. *B*, Graphics output from PolyWorks® software package showing point-cloud image of cutbank and geometric benchmarks. *C*, "Best-fit" sphere and cylinders. *D*, Reference points derived from the sphere center and the intersection of the cylinder axes.

Alignment of Sequential Surveys

The process of defining reference points was repeated for the seven geometric benchmarks in each survey. The seven reference points had the same spatial (geometric) relation, but the coordinate systems differed because the laser scanner was placed in a slightly different x , y , and z location during each survey. The alignment was accomplished by using the PolyWorks® software package, which rotates and translates the coordinate system of reference points from repeat surveys to that of the baseline survey. Errors associated with aligning arise from (1) minor misalignments in the baseline and repeat surveys, on the order of 4 to 6 mm; (2) variability in repositioning the reference spheres on the monuments, on the order of 2 to 4 mm; (3) variability in modeling the reference points for multiple study periods, on the order of less than

1 mm; and (4) monument instability, assumed to be negligible on the basis of physical inspections of the monuments, which remained stable and undisturbed during the entire study period.

Once a repeat survey was aligned to the baseline survey, an assessment of the alignment (quantitative error) was determined. This assessment accounts for the cumulative error from the various sources that were previously described. For each geometric benchmark (sphere or 'T') in the baseline and subsequent scans, the corresponding reference-point coordinates along the x , y , and z axes were tabulated and differenced. The variance along each axis, for each reference point, was used to calculate the RMSE of the alignment. The alignment of the second (January 2011) survey, relative to the baseline survey (the first survey, December 2010),

8 Quantifying Mercury-Contaminated Sediment at Stocking Flat, Deer Creek, Nevada County, Calif., 2010–13

produced a RMSE of 5.1 mm. For the third survey (May 2011), the RMSE was 5.7 mm, and for the fourth survey, the RMSE was 2.8 mm. The reference-point alignment technique used in this study resulted in a RMSE of the alignment (one-standard-deviation errors) on the order of 3 to 6 mm, which meant a 95-percent confidence interval, or a two-standard-deviation error, was equal to or less than 12 mm for these alignments. Precise 3-D measurements, discussed in the next section, comparing the stable geometric benchmarks in each survey confirmed the calculated 95-percent confidence interval of about 6- to 12-mm uncertainty in the alignment of sequential surveys.

Quality Assurance of Alignments

This study utilized the University of California, Davis (UCD) KeckCAVES (W.M. Keck Center for Active Visualization in the Earth Sciences) and the Virtual Reality User Interface (Vrui) LiDAR Viewer software (Kreylos and others, 2008) to visually inspect the lidar point-cloud data for the purpose of quality assurance (QA) of the alignment of overlapping scans from a single survey as well as the alignments of sequential surveys.

Immersion within lidar point-cloud data by utilizing 3-D virtual reality (VR) technologies offers a unique and powerful tool to visualize complex 3-D data sets that cannot be seen with a conventional two-dimensional (2-D) computer screen. At the UCD KeckCAVES, lidar point-cloud data are stereoscopically projected (with four projectors) onto the floor, back wall, and side walls of a square room (or “cave”), 3 m on each side. The projectors are linked to a head-tracked pair of eye glasses that enables 3-D visualization of the lidar point-cloud data in a virtual reality (VR), or fully immersive visualization environment. Using a hand-held controller, a user can move through the 3-D data, which can be enlarged to a scale greater than 1:1. The interactivity with the 3-D data enables the inspection and isolation of features more intuitively, quickly, and accurately than previously possible with non-immersive 2-D environments, such as desktop computers (Kellogg and others, 2008; Kreylos and others, 2008).

To verify the alignment of overlapping scans for a single survey, the data from each scan were color coded so that one scan could be easily differentiated from another. Within the area of overlap, features such as planar surfaces, distinctly shaped cobbles, and geometric benchmarks were isolated at a scale greater than or equal to 1:1. By clicking on common points with the hand-held controller, precise distances between overlapping scans were measured. These measurements were compared with the previously discussed statistical uncertainties generated by the alignment software to verify those values. Similarly, for the alignments of sequential surveys, each survey was color coded and distances between distinct points on the stable geometric benchmarks were measured, and the measured differences were compared to the previously discussed RMSE to verify those values.

Volumetric Determination

The PolyWorks® software package was used to determine the volume of cutbank erosion between sequential surveys: Surveys 1 and 2 (December 1, 2010, to January 20, 2011), Surveys 2 and 3 (January 20, 2011, to May 12, 2011), and Surveys 3 and 4 (May 12, 2011, to February 4, 2013). Before volumes could be determined between the surveys, additional steps were needed to remove unwanted points, to create surfaces from the remaining points, and to define a common perimeter.

Data-Point Removal

Areas of vegetation, scattered along the base and across the surface of the cutbank, were scanned during each survey (fig. 2B). Small clusters of vegetation (typically 0.5 m² in area) can create laser returns in front of the cutbank surface and also create “shadows” of missing data on the cutbank (blank areas in fig. 3C). Laser returns from vegetation were removed from the composite point cloud by using the software package TerraScan® (Version 12.020; Terrasolid, Helsinki, Finland), thus creating a bare-earth model of the cutbank surface. After the TerraScan® vegetation filter was applied to each survey, the data were subdivided into 2-m² areas. Each area was then individually inspected for stray laser returns that were not removed by the vegetation filter. Systematically inspecting the 2-m² areas ensured that points representing vegetation and other errant multipath laser returns were not included in the volume calculations.

Creating Surfaces

To calculate volume using the PolyWorks® software package requires that a continuous 3-D surface is generated from the land-surface points. Areas of missing data, caused by shadows from vegetation, protruding cobbles, or both, were interpolated by using two different techniques. The first technique, performed in PolyWorks®, transformed the lidar point cloud into a continuous 3-D surface by creating a triangulated irregular network (TIN) of nearest-neighbor points. A **kriging** algorithm (Surfer™ version 11.0, Golden Software, Inc., Golden, Colorado) was also used to generate a best-fit surface through the point cloud and to interpolate across areas of missing data. For each survey, volumes were calculated by using both types of surface (TIN and kriged) to assess differences in calculated volumes between the two techniques. The differences were less than 1 percent, and thus, either technique for this study was acceptable. Given the faster computational speed of generating a TIN surface (several minutes) compared to generating a kriged surface (tens of minutes), the TIN method for surface generation was preferred.

Defining a Common Boundary

Prior to calculating volume changes, the area of the data common to all surveys is needed. This step eliminates any effect of areal sampling bias on the calculated volume changes caused by a different extent of data among the surveys.

From a plan-view perspective, a common data boundary for the four surveys was defined across the upper terrace and along the upstream and downstream margins. Along these boundaries, data for the four surveys were trimmed to match the survey that had the least extent. Additional trimming along the water surface was also necessary because the stream's water-surface elevation was different during each of the surveys. The surveys with lower water surface were trimmed to that of the higher, so the lower data were not included in the volume calculation. The stream stage of the second survey was approximately 0.4 m lower than the stage of the first survey. Consequently, along the length of the cutbank, an area corresponding to the 0.4-m elevation difference was trimmed from the lower extent of the second survey to match the water-surface profile from the first survey. Similarly, for the second and third surveys, the stream stage of the second survey was approximately 0.2 m lower than the stage of the third survey, so the lowest 0.2 m of the second survey were excluded from the volume calculation. The fourth survey extended approximately 0.15 m lower than the third survey, so the lowest 0.15 m of the fourth survey were not included in the volume calculation.

This process normalizes the cutbank area to allow for a consistent comparison between the surveys. This normalization caused the subsequent volume-change calculations to be minima, because the volume of cutbank erosion below the higher of the two water-surface profiles was excluded in the erosion measurements.

The areal normalization of the sequential 3-D data sets was a straightforward process along the upper terrace, upstream margin, and downstream margin, and along the water-surface profile. Sparse point-cloud data directly next to the stream, however, required an interpretation of the lateral extent of the cutbank surface from a plan-view perspective. The sparse data density near the stream edge was caused by vegetation along the edge of the stream, which created

irregular data shadows (fig. 3C). Also, the wet alluvium along and above the creek's water surface attenuated the laser energy and prevented some of the laser pulses from returning to the scanner.

Two interpretive approaches were used to define the boundary (extent) of the data for each survey. In the first boundary approach, the landward extent of the data was used to define the edge of the cutbank, which created numerous apparent cavities in the cutbank along the edge of the stream. This first approach can underestimate the streamward extent of the cutbank if an apparent cavity was caused by a data shadow or attenuated laser returns. In the second boundary approach, the apparent cavities were bridged, which created a smoother edge along the cutbank and stream interface. This second approach can overestimate the streamward extent of the cutbank if an apparent cavity was actually a recess in the cutbank surface. For each survey, volumes were calculated by using both approaches with techniques described in the following section.

Calculating Volumetric Changes

The PolyWorks® software package was used to calculate the volume between a user-defined reference plane and a 3-D surface of the cutbank for each survey (fig. 6). The volume calculations for each survey were made relative to the same fixed-reference plane. The volumetric changes were computed by differencing the calculated volumes between sequential surveys. Because the PolyWorks® software calculates the volume perpendicular to the reference plane (fig. 6), the orientation of the reference plane was chosen to minimize volume "shadows" that could be created by the overhanging crest of the cutbank and by protruding cobbles. For this study, the reference plane was oriented approximately parallel to the length and slope of the cutbank and faced the concave side of the cutbank (fig. 6B). If a reference plane, for example, was set horizontally above the cutbank, the volume underneath the overhanging crest of the cutbank or under protruding cobbles would be missed. Because most Geographic Information System (GIS) software packages project data onto a horizontal plane, volumes would not be accurately calculated without an inclined reference plane.

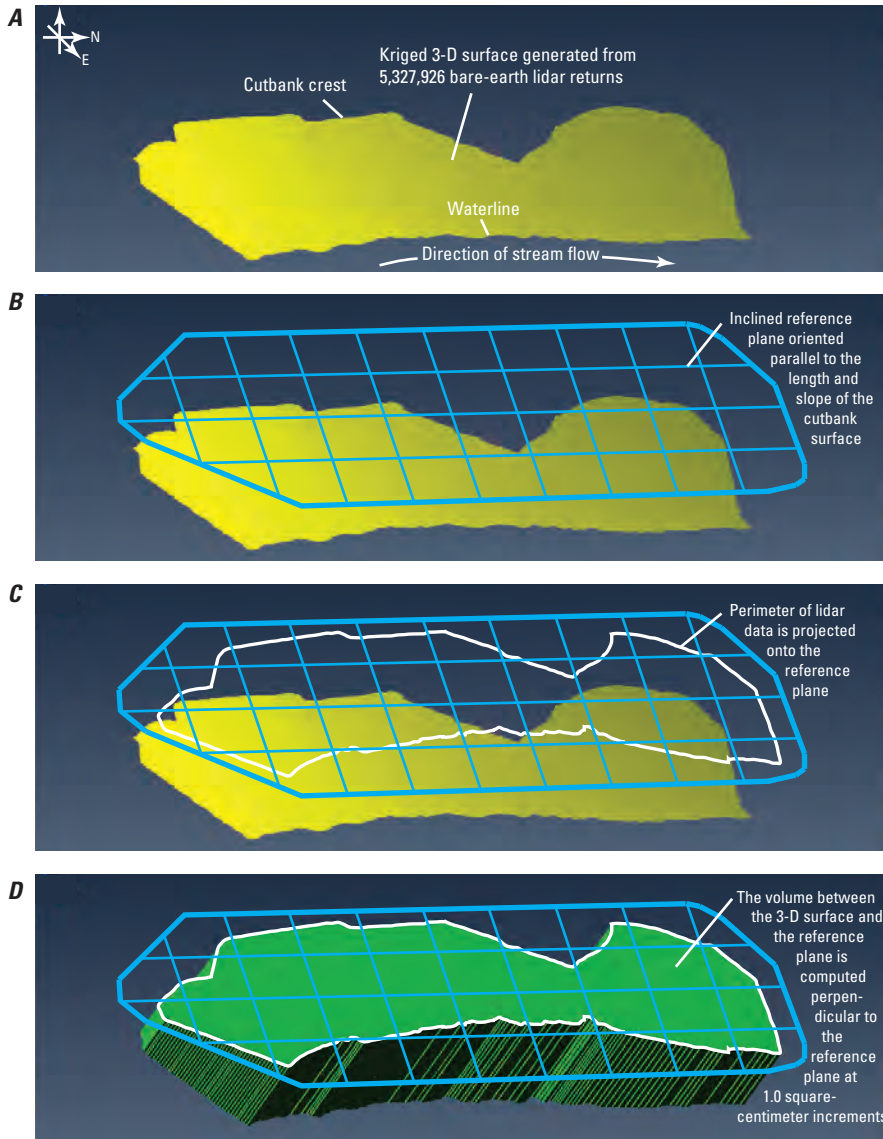


Figure 6. The sequence for calculating volume: *A*, oblique perspective, with view to west-northwest, showing kriged three-dimensional (3-D) surface of cutbank; horizontal distance along waterline is approximately 50 meters; *B*, reference plane used in volume calculation; *C*, perimeter of lidar (light detection and ranging) data projected onto the reference plane; and *D*, green polygon is the calculated volume between the surface of the cutbank and the reference plane.

Results of Volume Calculations

The previously discussed RMSE of the sequential alignments relative to the baseline survey (5.1 mm in January 2011, 5.7 mm in May 2011, and 2.8 mm in February 2013) were used to assess potential volumetric errors for the sequential alignments. The assessment was made by translating the reference plane along an axis perpendicular to the reference plane by plus or minus the RMSE value and calculating surface-to-plane volumes that bracket the volume calculated with the fixed-reference plane (table 1). Translating the reference plane by one RMSE in the positive direction (toward the cutbank surface) resulted in a smaller calculated volume (fig. 7; table 1). Conversely, translating the reference

plane by one RMSE in the negative direction (away from the cutbank) resulted in a larger calculated volume. Note that alignment errors parallel to the reference plane did not change the calculated volume and that the largest potential errors were generated from misalignments that are perpendicular to the reference plane. The calculated volumes (plus or minus one RMSE) spanned a range equivalent to the 95-percent confidence interval (two standard deviation error) for each sequential alignment. These volumetric error assessments were made both for the first and for the second boundary-approach data sets (table 1). Note that for any given survey, the first boundary approach, or interpretation, of the stream edge with cavities yielded a larger surface-to-plane volume than the second boundary approach, or interpretation, which had a smoother stream edge (fig. 7).

By using data sets with the first and second boundary approaches and reference planes adjusted for potential alignment error, volumes for each period were calculated by using a discretization interval of 1.0 square centimeter (cm²). This discretization interval was integrated across the entire area of the cutbank surface (fig. 6D), which produced a high-resolution surface-to-plane volume measurement (table 1). The volume changes (erosion measurements) for each period (December 2010 to January 2011, January 2011 to May 2011, and May 2011 to February 2013), were computed by differencing the calculated volumes for the two surveys that bracket a given period. The calculated volume of eroded sediment for each period represented the 3-D space between the cutbank surfaces for the surveys bracketing that period.

For each period, a range of volume changes were calculated by differencing end-member values derived from the first and second boundary-approach data sets and associated alignment errors (table 1). For example, to estimate the maximum amount of erosion for the January 2011 to May 2011 period, the second boundary-approach January data (with a positive reference-plane error) were subtracted from the first boundary-approach May data (with a negative reference-plane error). Conversely, to estimate the minimum amount of erosion for the January 2011 to May 2011 period, the first boundary-approach January data (with a negative reference-plane error) were subtracted from the second boundary-approach May data (with a positive reference-plane error). Averaged results of these combinations and the range of uncertainties are discussed in the following paragraphs.

Table 1. Calculated volumes between the cutbank surface and reference planes for surveys 1, 2, 3, and 4.

[Volumes were calculated using both the first (Model A) and second (Model B) boundary interpretations of the stream edge, the fixed reference plane, and reference planes adjusted plus and minus (±) one root mean square error (RMSE) relative to the fixed reference plane. **Abbreviations:** m³, cubic meters; Survey 1, December 1, 2010; Survey 2, January 20, 2011; Survey 3, May 12, 2011; Survey 4, February 4, 2013; —, no data]

| Survey and stream-edge interpretation (Model A or Model B) | Volume between fixed reference plane and cutbank surface (m ³) | Volume between reference plane (adjusted plus one RMSE) and cutbank surface (m ³) | Volume between reference plane (adjusted minus one RMSE) and cutbank surface (m ³) | Range in volume from ± RMSE (m ³) | Erosion volume from Dec. 1, 2010, to Jan. 20, 2011 (m ³) |
|--|--|---|--|---|--|
| Model A ¹ | | | | | |
| Survey 1 | 2,008 | ² 2,008 | ² 2,008 | 0 | — |
| Survey 2 | 2,146 | ^{3,4} 2,144 | ^{3,5} 2,148 | ±2 | — |
| Model B ⁶ | | | | | |
| Survey 1 | 1,990 | ² 1,990 | ² 1,990 | 0 | — |
| Survey 2 | 2,138 | ³ 2,136 | ³ 2,139 | ±2 | — |
| Maximum erosion | — | — | — | — | ⁷ 158 |
| Minimum erosion | — | — | — | — | ⁸ 128 |
| Average erosion and range of uncertainty | — | — | — | — | 143 ±15 |
| Survey and stream-edge interpretation (Model A or Model B) | Volume between fixed reference plane and cutbank surface (m ³) | Volume between reference plane (adjusted plus one RMSE) and cutbank surface (m ³) | Volume between reference plane (adjusted minus one RMSE) and cutbank surface (m ³) | Range in volume from ± RMSE (m ³) | Erosion volume from Jan. 20, 2011, to May 12, 2011 (m ³) |
| Model A ¹ —Continued | | | | | |
| Survey 2 | ⁹ 2,382 | ³ 2,380 | ³ 2,384 | ±2 | — |
| Survey 3 | 2,582 | ¹⁰ 2,580 | ¹⁰ 2,584 | ±2 | — |
| Model B ⁶ —Continued | | | | | |
| Survey 2 | ⁹ 2,355 | ³ 2,353 | ³ 2,357 | ±2 | — |
| Survey 3 | 2,569 | ¹⁰ 2,567 | ¹⁰ 2,571 | ±2 | — |
| Maximum erosion | — | — | — | — | ¹¹ 231 |
| Minimum erosion | — | — | — | — | ¹² 183 |
| Average erosion and range of uncertainty | — | — | — | — | 207 ±24 |

12 Quantifying Mercury-Contaminated Sediment at Stocking Flat, Deer Creek, Nevada County, Calif., 2010–13

Table 1. Calculated volumes between the cutbank surface and reference planes for surveys 1, 2, 3, and 4.—Continued

[Volumes were calculated using both the first (Model A) and second (Model B) boundary interpretations of the stream edge, the fixed reference plane, and reference planes adjusted plus and minus (\pm) one root mean square error (RMSE) relative to the fixed reference plane. **Abbreviations:** m³, cubic meters; Survey 1, December 1, 2010; Survey 2, January 20, 2011; Survey 3, May 12, 2011; Survey 4, February 4, 2013; —, no data]

| Survey and stream-edge interpretation (Model A or Model B) | Volume between fixed reference plane and cutbank surface (m ³) | Volume between reference plane (adjusted plus one RMSE) and cutbank surface (m ³) | Volume between reference plane (adjusted minus one RMSE) and cutbank surface (m ³) | Range in volume from \pm RMSE (m ³) | Erosion volume from May 12, 2011, to Feb. 4, 2013 (m ³) |
|--|--|---|--|---|---|
| Model A ¹ —Continued | | | | | |
| Survey 3 | 2,582 | ¹⁰ 2,580 | ¹⁰ 2,584 | ± 2 | — |
| Survey 4 | 2,594 | ¹³ 2,593 | ¹³ 2,595 | ± 1 | — |
| Model B ⁶ —Continued | | | | | |
| Survey 3 | 2,569 | ¹⁰ 2,567 | ¹⁰ 2,571 | ± 2 | — |
| Survey 4 | 2,593 | ¹³ 2,592 | ¹³ 2,594 | ± 1 | — |
| Maximum erosion | — | — | — | — | ¹⁴ 28 |
| Minimum erosion | — | — | — | — | ¹⁵ 8 |
| Average erosion and range of uncertainty | — | — | — | — | 18 \pm 10 |

¹The calculated volume of the “Model A” data set (first boundary approach or interpretation of the stream edge), for any given timeframe, is larger than the calculated volume of the “Model B” data set (second boundary approach) for the same timeframe, because the cavities along the waterline create a larger volume between the cutbank surface and the reference plane. See discussion in [Defining a Common Boundary](#) section of report and [figure 7](#).

²The baseline survey on December 1, 2010, was held fixed; reference plane adjustments were only made for subsequent surveys, which were compared to the baseline survey. See discussion in [Alignment of Sequential Surveys](#) section of report.

³The root mean square alignment error (RMSE) of the January 2011 survey relative to the baseline survey was 5.1 millimeters (mm). See discussion in [Alignment of Sequential Surveys](#) section of report.

⁴Translating the reference plane by one RMSE in the positive direction (toward the cutbank surface) resulted in a smaller calculated volume. See discussion in [Calculating Volumetric Changes](#) section of report and [figure 7](#).

⁵Translating the reference plane by one RMSE in the negative direction (away from cutbank surface) resulted in a larger calculated volume. See discussion in [Calculating Volumetric Changes](#) section of report and [figure 7](#).

⁶The calculated volume of a “Model B” data set, for any given timeframe, was smaller than the calculated volume of the “Model A” data set for the same timeframe, because the apparent cavities along the waterline were bridged creating less volume between the cutbank surface and the reference plane. See discussion in [Defining a Common Boundary](#) section of report and [figure 7](#).

⁷The maximum erosion from December 2010 to January 2011 is the difference between the January 2011 “Model A” (minus one RMSE) volume and the December 2010 “Model B” (plus one RMSE) volume. See discussion in [Calculating Volumetric Changes](#) section of report and [figure 7](#).

⁸The minimum erosion from December 2010 to January 2011 is the difference between the January 2011 “Model B” (plus one RMSE) volume and the December 2010 “Model A” (minus one RMSE) volume. See discussion in [Calculating Volumetric Changes](#) section of report and [figure 7](#).

⁹The calculated volume for January 2011 that was compared to May 2011 was larger than the January 2011 volume that was compared to December 2010, because the May 2011 water profile was lower than the December 2010 water profile, which allowed for a greater extent of the January 2011 data to be used for comparison. See discussion in [Defining a Common Boundary](#) section of report.

¹⁰The RMSE of the May 2011 survey relative to the baseline survey was 5.7 mm. See discussion in [Alignment of Sequential Surveys](#) section of report.

¹¹The maximum erosion from January 2011 to May 2011 is the difference between the May 2011 “Model A” (minus one RMSE) volume and the January 2011 “Model B” (plus one RMSE) volume.

¹²The minimum erosion from January 2011 to May 2011 is the difference between the May 2011 “Model B” (plus one RMSE) volume and the January 2011 “Model A” (minus one RMSE) volume.

¹³The RMSE of the February 2013 survey relative to the baseline survey was 2.8 mm. See discussion in [Alignment of Sequential Surveys](#) section of report.

¹⁴The maximum erosion from May 2011 to February 2013 is the difference between the February 2013 “Model A” (minus one RMSE) volume and the May 2011 “Model B” (plus one RMSE) volume.

¹⁵The minimum erosion from May 2011 to February 2013 is the difference between the February 2013 “Model B” (plus one RMSE) volume and the May 2011 “Model A” (minus one RMSE) volume.

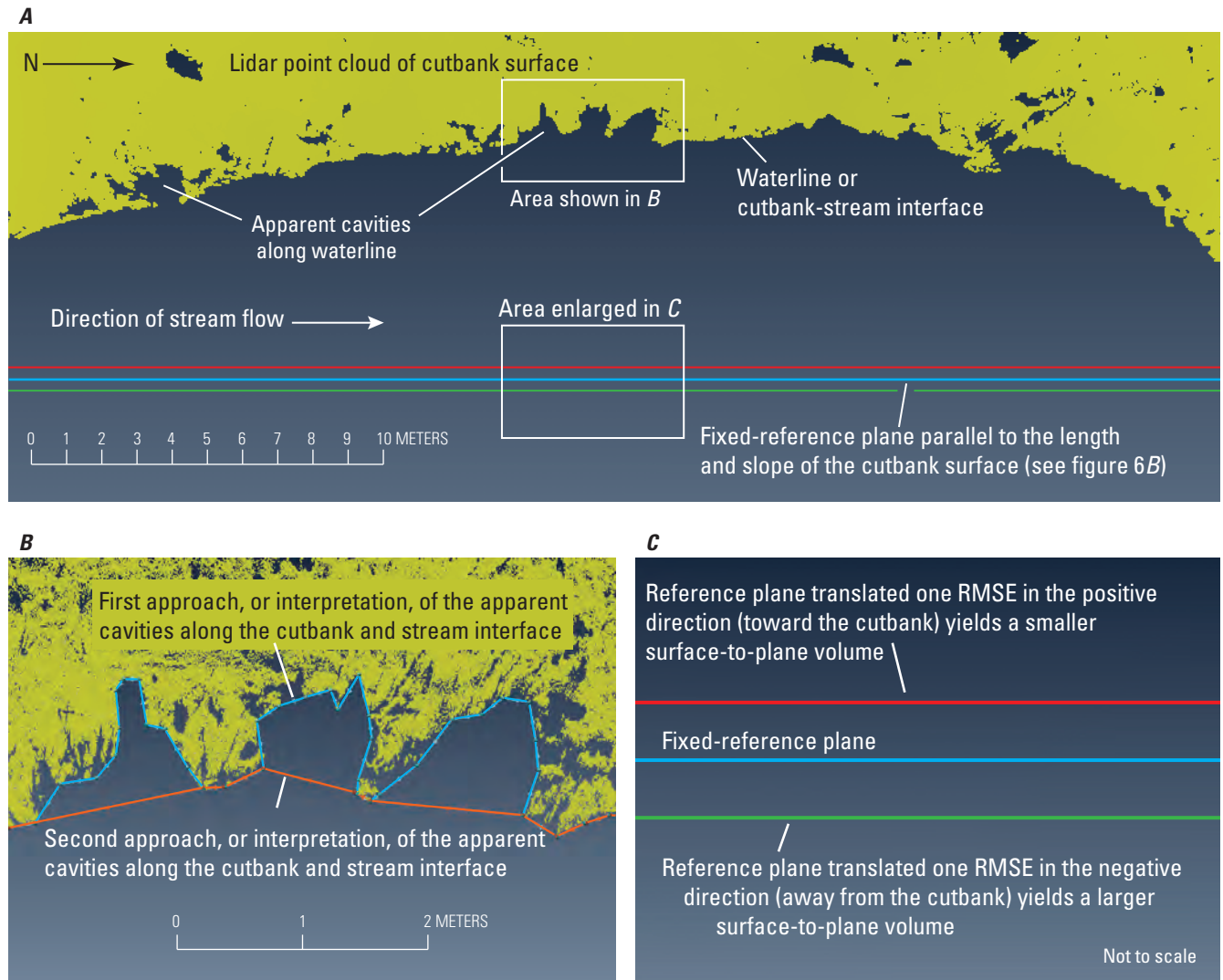


Figure 7. Lidar point cloud of the cutbank surface: *A*, oblique view, parallel to the fixed-reference plane, showing areas of apparent cavities along the waterline; *B*, first and second boundary approaches, or interpretations, of the apparent cavities along the cutbank and stream interface; and *C*, positions of reference planes translated plus and minus one root-mean-square alignment error (RMSE) value relative to the fixed-reference plane.

For the three periods, the range in the uncertainty values, plus or minus relative to the average (plus or minus 15 m^3 , plus or minus 24 m^3 , and plus or minus 10 m^3), reflected the range of values likely to contain the average value (tables 1, 2). The range of values for each period was derived by combining subjective interpretations (first and second boundary approaches to define the edge of the cutbank along the waterline) coupled with objective error assessments of the sequential alignments. Although the objective volumetric error associated with sequential alignments can be quantified in terms of a 95-percent confidence interval, the subjective error cannot be quantified in terms of a confidence interval.

Between the first survey (December 1, 2010) and second survey (January 20, 2011), a minimum of 143 plus or minus 15 m^3 of Hg-contaminated sediment was eroded from the Stocking Flat cutbank study site. Between the second survey (January 20, 2011) and third survey (May 12, 2011), at

least 207 plus or minus 24 m^3 of sediment were eroded from the cutbank. Adding these two estimates, the total estimated volume of Hg-contaminated sediment eroded by Deer Creek for the period from December 1, 2010, to May 12, 2011, was greater than 350 plus or minus 28 m^3 (table 2). Between the third and fourth surveys (May 12, 2011, to February 4, 2013), an additional 18 plus or minus 10 m^3 of Hg-contaminated sediment was eroded.

For the three periods during the study (December 2010 to January 2011, January 2011 to May 2011, and May 2011 to February 2013), the total average volume of eroded material was at least 368 plus or minus 30 m^3 (table 2). This erosion volume is a minimum, because during each period, the volume of cutbank erosion below the higher of the two water-surface profiles was excluded from the erosion measurements, as previously discussed.

Visualization of Changes

The purpose of this section is to demonstrate that visualization can reveal important insights into the data. Tufte (1983) stated, “*Graphics are instruments for reasoning about quantitative information. Often the most effective way to describe, explore, and summarize a set of numbers—especially a very large set—is to look at pictures of those numbers.*” Also, Kellogg and others (2008) noted, “*The human brain excels at visually identifying patterns, and as a result, the best interpretations arise when scientists can fully visualize their data.*”

In this section, the three dimensionality of the lidar data used in this study is demonstrated by a combination of shaded-relief images, 2-D change maps, and 3-D anaglyphs. The various techniques allowed for the visualization of where, when, and how much the cutbank changed. The graphics can also provide insights regarding the interpretation of the processes responsible for the observed changes and where mitigation measures can be most effective.

Shaded-Relief Images

The first visualization technique is a shaded-relief image with color-coded elevation and artificial illumination (fig. 8), which was generated by using the Quick Terrain Modeler™ software (QT Modeler, Version 7.0.2, Applied Imagery, Silver Spring, Maryland). This technique was performed on each of the four surveys. An oblique view was used to permit a view of the entire cutbank and upper terrace. This oblique perspective was maintained for all surveys to allow one to easily see changes from one image to the next. Artificial illumination was also used to highlight subtle geomorphic features that provide insight to the slope processes at work.

The first survey (December 1, 2010) showed a generally uniform slope across the cutbank surface at or near the **angle of repose** (fig. 8A). The artificial illumination cast a

dark shadow where an over-hanging free face had formed at the upstream end of the cutbank crest. Also, a lobe of **colluvium** protruded along the waterline of the stream near the downstream end of the cutbank.

By January 20, 2011 (second survey), the protruding lobe of colluvium was eroded by the stream (fig. 8B). This erosion, which took place between the first and second surveys, was primarily along the down-stream half of the cutbank, where arcuate head scarps also formed in the unconsolidated sediment. The head scarps were interpreted to be the product of rotational slumping, which was most likely induced by stream under-cutting of water-saturated sediment. Also, between the first and second surveys, erosion of the cutbank crest caused the over-hanging free face to become less steep (near vertical), which is evident by the brighter illumination of the free face shown in figure 8B compared with figure 8A.

During March 2011, a period of high streamflow (fig. 9) caused substantial erosion along the entire lower part of the cutbank. This erosion formed a near-vertical fluvial scarp along the length of the cutbank (fig. 8C), which destabilized the unconsolidated sediment on the upper part of the cutbank and initiated the down-slope transport of sediment (fig. 9). By the time of the third survey (May 12, 2011), the near-vertical fluvial scarp had been partially buried by the down-slope movement of sediment (fig. 8C). The down-slope transport of sediment caused localized lowering of the cutbank crest and also caused the enlargement and over-steepening of the previously mentioned free face near the upstream end of the cutbank (fig. 8C). Most of the down-slope transport of sediment, from the destabilized upper part of the cutbank, likely was accomplished by gravity-driven **dry ravel**. Near the downstream end of the cutbank, however, a translational slope failure also appears to have occurred; this interpretation was based on a shallow and arcuate head scarp near the crest of the cutbank, a relatively smooth and flat surface directly below it, and an irregular and chaotic accumulation of sediment farther down the slope (fig. 8C).

Table 2. Measured volumes of mercury-contaminated sediment (in cubic meters) eroded from the Stocking Flat cutbank study site for various periods between December 1, 2010, and February 4, 2013.

[±, plus or minus]

| Surveys | Time span | Days | Minimum erosion volume (cubic meters) | Uncertainty (cubic meters) |
|-----------------|--|------|---------------------------------------|----------------------------|
| 1–2 | December 1, 2010, to January 20, 2011 | 50 | 143 | ±15 |
| 2–3 | January 20, 2011, to May 12, 2011 | 112 | 207 | ±24 |
| Sub-total (1–3) | Erosion from December 1, 2010, to May 12, 2011 | 162 | 350 | ¹ ±28 |
| 3–4 | May 12, 2011, to February 4, 2013 | 634 | 18 | ±10 |
| Total (1–4) | Total erosion from December 1, 2010, to February 4, 2013 | 796 | 368 | ² ±30 |

¹The cumulative uncertainty of the erosion volume, in cubic meters (m³), for the December 2010 to May 2011 subtotal was calculated with the following equation: Cumulative Error (CE) = √(Survey 1–2 uncertainty)² + (Survey 2–3 uncertainty)² or CE = √(15)² + (24)² = 28 m³.

²The cumulative uncertainty of the erosion volume (in cubic meters) for the December 2010 to February 2013 total was calculated with the following equation: CE = √(Surveys 1–2 uncertainty)² + (Surveys 2–3 uncertainty)² + (Surveys 3–4 uncertainty)² or CE = √(15)² + (24)² + (10)² = 30 m³.

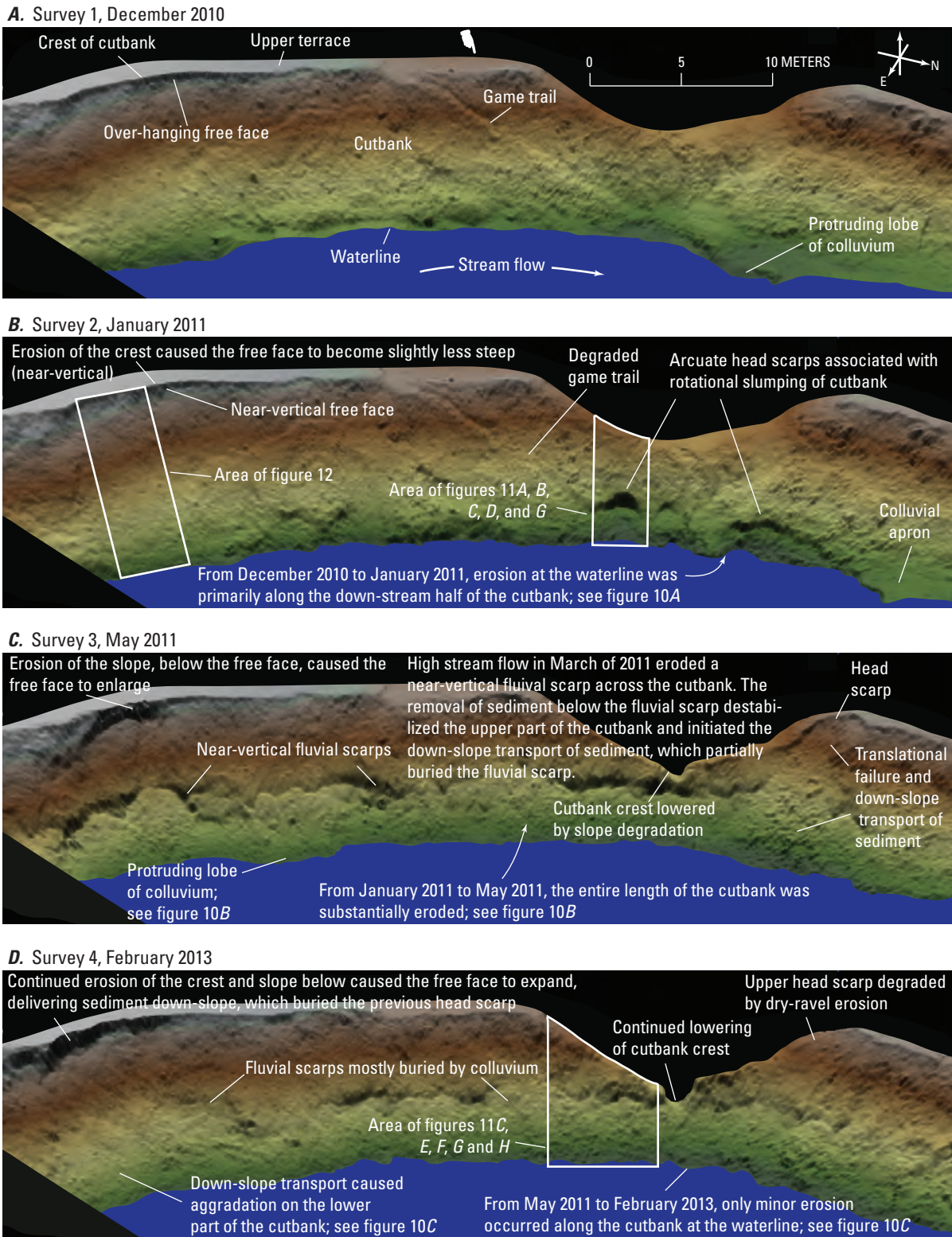


Figure 8. Shaded-relief oblique views of Stocking Flat cutbank study site near Nevada City, California, for the four surveys between December 2010 and February 2013. The images were created with Quick Terrain Modeler™ software (QT Modeler, Version 7.0.2, Applied Imagery, Silver Spring, Maryland). Points of equal elevation are color coded. The hand icon shows artificial illumination direction from the southwest. The upper terrace (bright gray) is approximately 8 meters above the waterline. The oblique perspective and illumination are the same for all images. *A*, Survey 1: December 1, 2010; *B*, Survey 2: January 20, 2011; *C*, Survey 3: May 12, 2011; and *D*, Survey 4: February 4, 2013.

Between the third and fourth surveys (from May 12, 2011, to February 4, 2013), the unsupported upper part of the cutbank, above the partially buried fluvial scarps shown in [figure 8C](#), continued to erode and deliver sediment down slope. This down-slope transport of sediment mostly buried the remaining fluvial scarps formed during March of 2011 ([fig. 8D](#)). The continued down-slope transport caused further lowering of the cutbank crest and the expansion of the near-vertical free face at the upstream end of the cutbank ([fig. 8D](#)). During this final period, there was only minor erosion along the waterline at the base of the cutbank.

Two-Dimensional Change Maps

The second visualization technique uses color-coded, 2-D change maps, which were created by using the PolyWorks® software package to measure the distance between the sequential data along the horizontal axis, perpendicular to the image. These images show the amount and spatial variability of change across the entire cutbank surface between sequential surveys ([fig. 10](#)) and for discrete areas of the cutbank ([figs. 11B, D, F, H, 12B–D](#)). These images also demonstrate the centimeter-scale resolution of the TLS data. By comparing the oblique-perspective shaded-relief images to the color-coded change maps for the same period, the viewer can acquire a more comprehensive picture of where and how much changed during a given period.

For example, the protruding lobe of colluvium shown in the first survey ([fig. 8A](#); December 1, 2010) had been removed by stream erosion by the time of the second survey ([fig. 8B](#); January 20, 2011). The amount of horizontal change

(erosion) during the period varied from approximately 2 m to approximately 3.5 m along the section of the waterline where the apron of colluvium was eroded ([fig. 10A](#)).

Between the second and third surveys (from January 20, 2011, to May 12, 2011), high streamflow during March 2011 ([fig. 9](#)) resulted in substantial erosion along the entire lower part of the cutbank ([fig. 10B](#)) and the formation of a fluvial scarp ([fig. 8C](#)). The broad area of yellow to orange across the lower half of the cutbank in [figure 10B](#) represents horizontal erosion ranging from approximately 2 to 2.5 m between the second and third surveys. The upper extent of the yellow to orange areas generally correlates with the top of the fluvial scarp eroded in March of 2011. In [figure 10B](#), the upper part of the cutbank has a green to yellow color gradation that represents horizontal erosion of approximately 0.5 to 1.5 m. This erosion across the upper part of the cutbank was caused by down-slope transport of sediment (dry ravel) after the formation of the fluvial scarp, which destabilized the upper part of the cutbank.

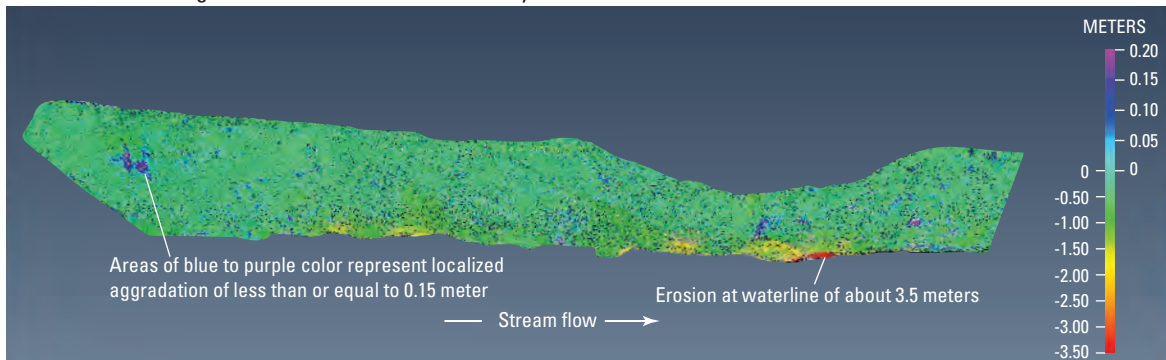
[Figure 10C](#) shows the horizontal change between the third and fourth surveys (from May 12, 2011, to February 4, 2013). During this period, erosion continued across the upper part of the cutbank, while there was generally deposition across the lower part. This was most notable at the upstream end of the cutbank, where an area of erosion that exceeded 1.0 m into the slope resulted in down-slope transport of sediment and deposition over a similar-sized area as was eroded ([fig. 10C](#)). The erosion on the upper part of the slope caused the free face to expand in size, and the down-slope transport of the sediment buried the fluvial scarp that was visible in May of 2011 with colluvium ([figs. 8C, D](#)).



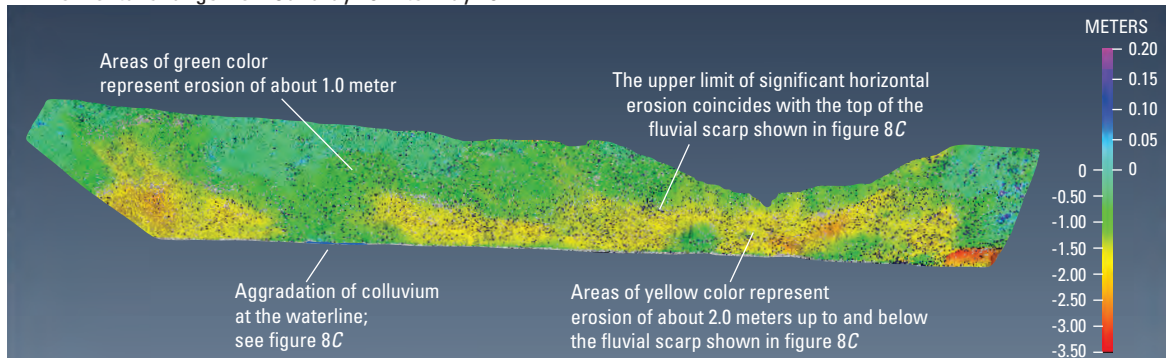
Photograph by Carrie Monohan

Figure 9. The central part of the cutbank on March 17, 2011, high streamflow and the near-vertical fluvial scarp.

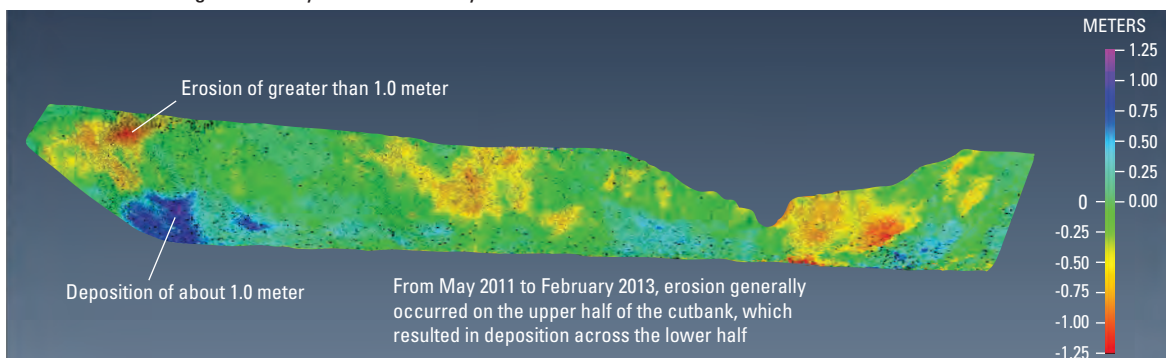
A. Horizontal change from December 2010 to January 2011



B. Horizontal change from January 2011 to May 2011



C. Horizontal change from May 2011 to February 2013



D. Horizontal change from December 2010 to February 2013

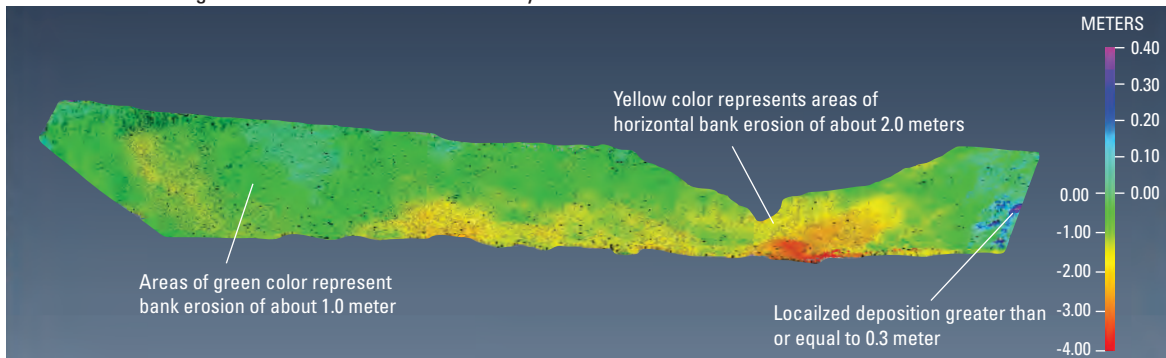
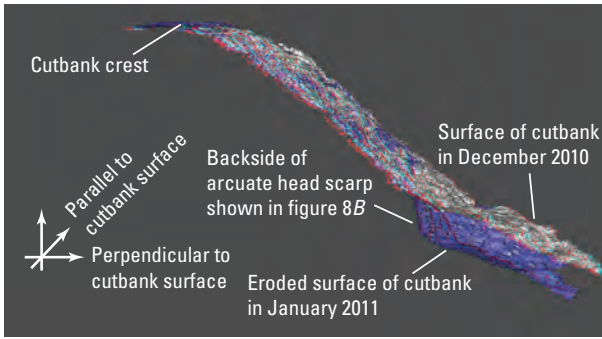


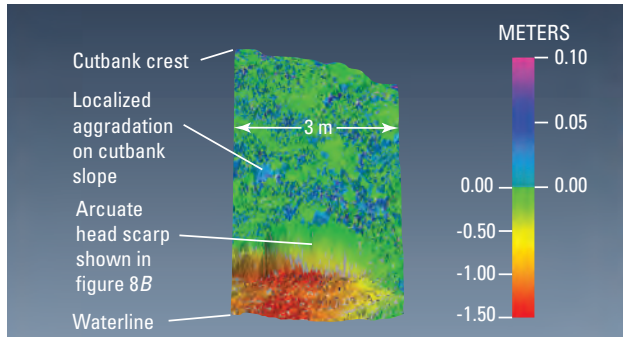
Figure 10. Difference maps of horizontal change across the cutbank surface for four periods between December 1, 2010, and February 4, 2013. All images are from a horizontal perspective, with a view to the west-southwest, and the distance along the base of the cutbank was approximately 50 meters. Changes, in meters, were measured perpendicular to the image. *A*, December 1, 2010, to January 20, 2011; *B*, January 20, 2011, to May 12, 2011; *C*, May 12, 2011, to February 4, 2013; and *D*, December 1, 2010, to February 4, 2013.

18 Quantifying Mercury-Contaminated Sediment at Stocking Flat, Deer Creek, Nevada County, Calif., 2010–13

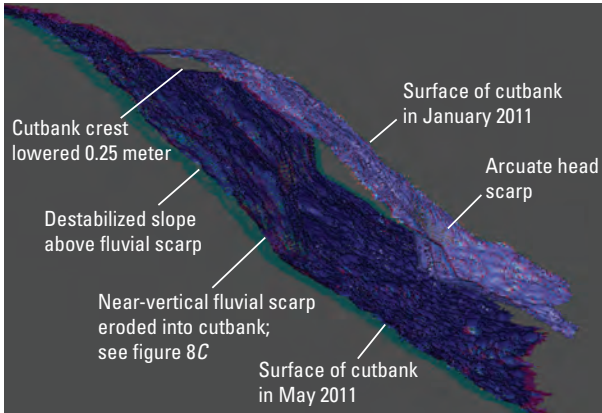
A. December 2010 and January 2011



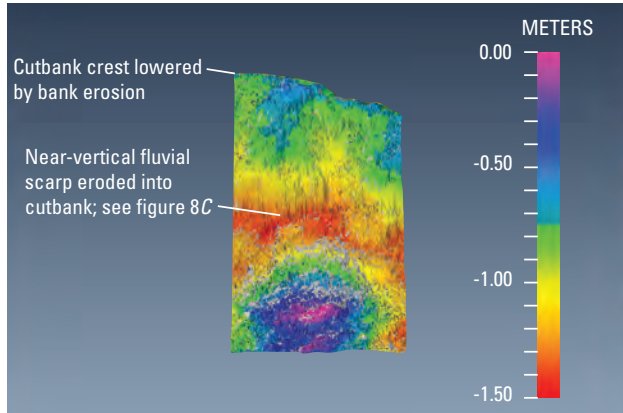
B. Change from December 2010 to January 2011



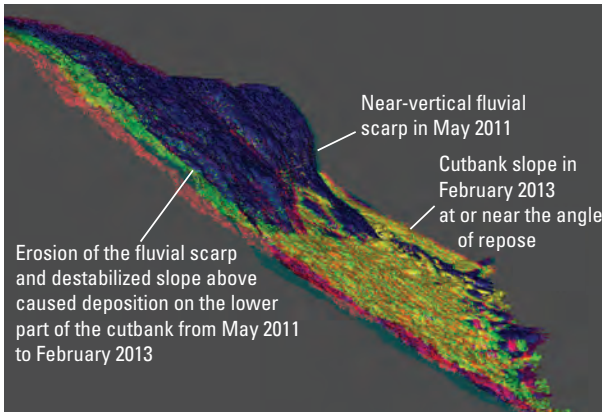
C. January 2011 and May 2011



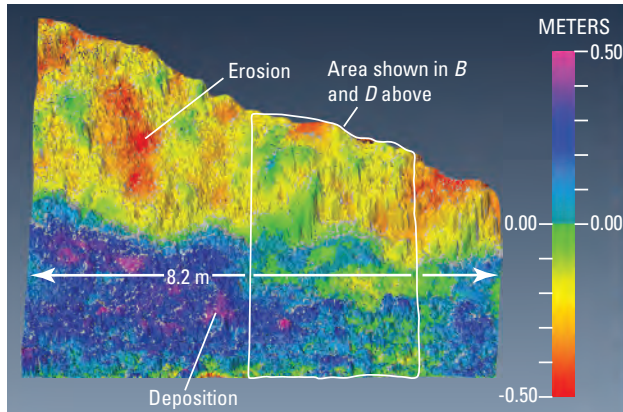
D. Change from January 2011 to May 2011



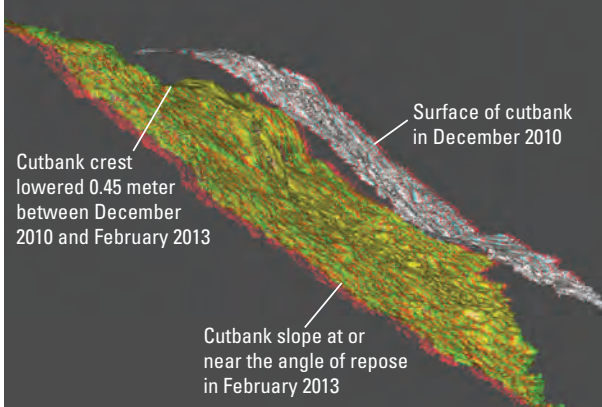
E. May 2011 and February 2013



F. Change from May 2011 to February 2013



G. December 2010 and February 2013



H. Change from December 2010 to February 2013

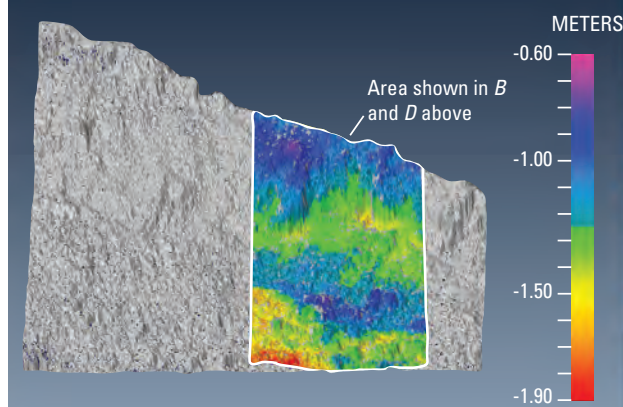


Figure 11. Three-dimensional (3-D) anaglyphs and two-dimensional (2-D) difference maps showing changes from December 2010 to February 2013 for selected areas of the cutbank. Inset images *A*, *C*, *E*, and *G* are oblique-perspective 3-D anaglyphs showing a sequence of the retreating cutbank. The oblique perspective, looking downstream, is the same for all images. Red-blue glasses (with the red lens on the right side) are needed for enhanced 3-D viewing. Anaglyphs were generated with Vrui LiDAR Viewer software. Inset images *B*, *D*, *F*, and *H* are graphics from PolyWorks® software showing 2-D color-coded difference maps of the same areas and time frames shown in the neighboring anaglyphs. Changes, in meters, were measured perpendicular to the image. *A*, Oblique anaglyph comparing a selected area of the cutbank from December 2010 and January 2011. See figure 8B for location of selected area. *B*, Difference map of data shown in *A*. *C*, Oblique anaglyph comparing selected areas of the cutbank in January 2011 and May 2011. See figure 8D for areal extent and location of May 2011 data. *D*, Difference map of data shown in *C*. This difference map only covers the areal extent of the January 2011 data. *E*, Oblique anaglyph comparing selected areas of the cutbank in May 2011 and February 2013. See figure 8D for extent and location of selected area. *F*, Difference map of data shown in *E*. *G*, Oblique anaglyph comparing selected areas of the cutbank in December 2010 and February 2013. See figure 8D for extent and location of selected area. *H*, Difference map of data shown in *G*. This difference map only covers the area of union for the December 2010 and February 2013 data.

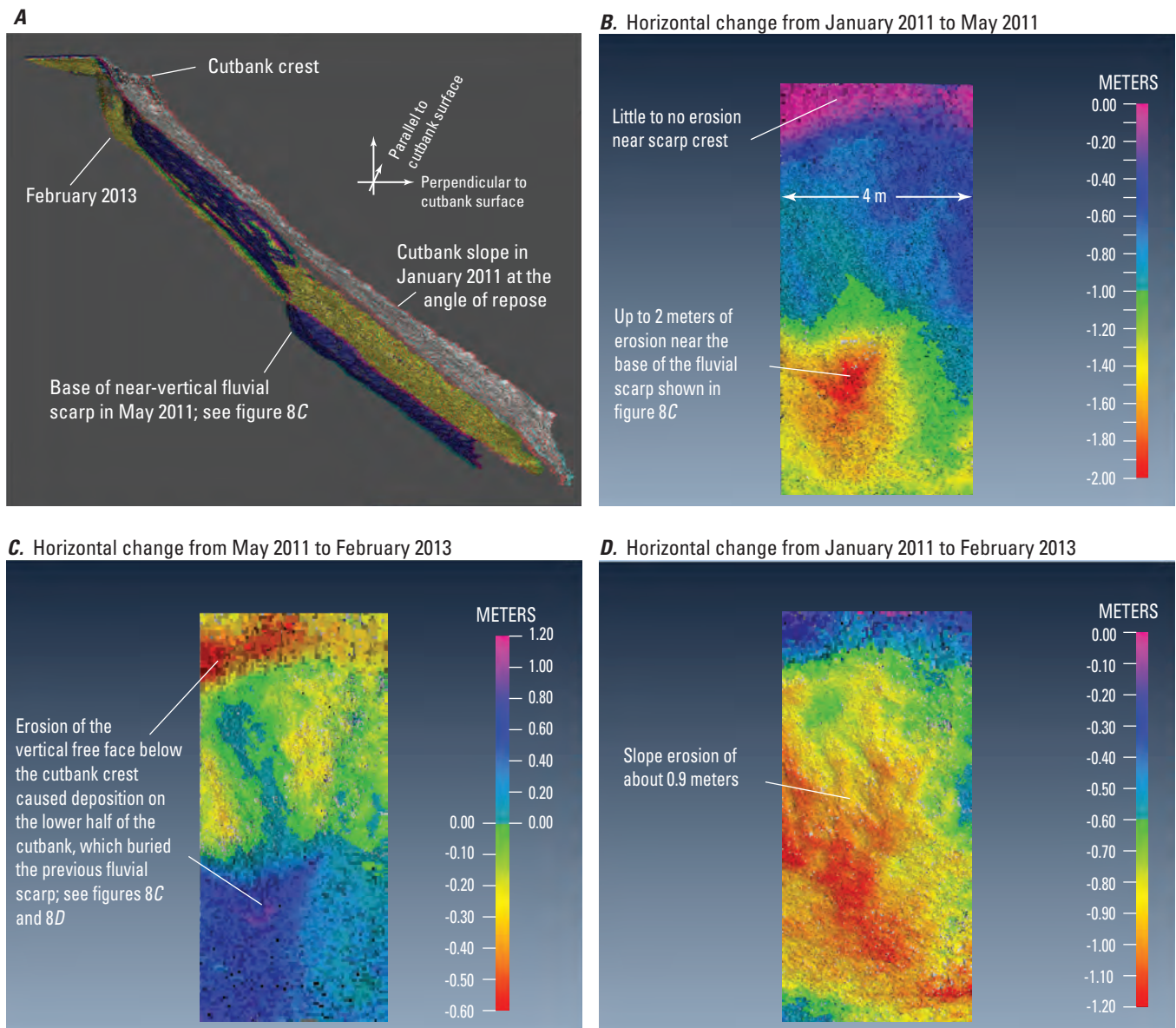


Figure 12. Three-dimensional (3-D) anaglyph and two-dimensional (2-D) difference maps showing changes from January 2011 to February 2013 for a selected area of the cutbank. See figure 8B for location of the selected area. *A*, Oblique-perspective 3-D anaglyph, looking downstream, shows a sequence of the retreating cutbank from January 2011, May 2011, and February 2013. Red-blue glasses (with the red lens on the right side) are needed for enhanced 3-D viewing. Anaglyphs were generated with Vrui LiDAR Viewer software. *B*, Graphic output from PolyWorks® software showing 2-D difference map for the period January 2011 to May 2011 for the area shown in *A*. Changes, in meters, were measured perpendicular to the image. Note that the color scales are different for figures *B*, *C*, and *D*. *C*, Difference map of data shown in *A* for the period May 2011 to February 2013. *D*, Difference map of data shown in *A* for the period January 2011 to February 2013.

Figure 10D shows the overall horizontal change between the first and last surveys (from December 1, 2010, to February 4, 2013). During the study period, the greatest amount of erosion was near the downstream end of the cutbank, where the horizontal change approached 4.0 m. This area of greatest erosion along the waterline corresponded in space with the greatest amount of cutbank-crest lowering (figs. 8A, D, 10A, C) as a result of the undermining of the slope base by stream erosion.

Three-Dimensional Anaglyphs

The third technique used to visualize 3-D changes of the sequential data is oblique-perspective anaglyphs. An **anaglyph image** is a stereoscopic 3-D effect that provides the viewer with the perception of depth (figs. 11A, C, E, G, 12A). By using Vruil LiDAR Viewer software (Kreylos and others, 2008), the 3-D effect is achieved by encoding images with different colors for each eye. When viewed through the color-coded anaglyph glasses (red and blue lens glasses), each of the images reaches one eye, giving perception of a 3-D scene. The oblique perspective of selected areas of the cutbank allows the viewer to visualize the space between sequential lidar data. By comparing an oblique-perspective anaglyph to the 2-D color-coded change map (for example, figs. 11A, B), the viewer can see the relative positions of the cutbank at different times in the anaglyph and also see a quantitative measure of the intervening space in the 2-D color-coded change map.

Figure 11A shows an oblique-perspective anaglyph, looking downstream, for a selected 3-m-wide swath of the cutbank on December 1, 2010, and January 20, 2011 (see fig. 8B for location of the selected area). Between the first and second surveys, there were only minor localized changes across the upper part of the cutbank (fig. 11B). At the base of the cutbank, however, an arcuate-shaped head scarp formed in the unconsolidated sediment (figs. 8B, 11A). The head scarp, a product of rotational slumping, caused localized erosion of 1.5 m into the cutbank (fig. 11B).

The 3-D anaglyph in figure 11C has the same oblique perspective and data from January 2011 as figure 11A, as well as an 8-m-wide area of data from May of 2011 (see fig. 8D for the location and extent of the May 2011 data). Between the January 20, 2011, and May 12, 2011, surveys, a period of high streamflow during mid-March (fig. 9) caused substantial erosion of the cutbank and formed a near-vertical fluvial scarp (fig. 11C, D). After the near-vertical fluvial scarp formed, the slope above it became destabilized, which initiated the down-slope transport of sediment. From May 2011 to February 2013, the unsupported fluvial scarp and upper part of the cutbank locally eroded as much as 0.5 m, resulting in localized deposition of 0.5 m on the lower half of the cutbank (fig. 11F).

From December 2010 to February 2013, the maximum horizontal erosion at the base of the cutbank was approximately 1.9 m within the area of data overlap (fig. 11H).

Near the top of the cutbank, the horizontal erosion totaled approximately 1.0 m (fig. 11H), which resulted in the crest of the cutbank being lowered approximately 0.45 m (fig. 11G).

Figure 12A shows an oblique perspective anaglyph, looking downstream, for a selected 4-m-wide swath of the cutbank for three dates: January 20, 2011; May 12, 2011; and February 4, 2013 (see fig. 8B for the location of the selected area). In January 2011, the cutbank slope was at or near the angle of repose, with a slightly over-steepened section below the crest (fig. 12A). The high streamflow in March 2011 (fig. 9) cut a near-vertical fluvial scarp and caused horizontal erosion of approximately 2.0 m near the base of fluvial scarp (fig. 12B). After the formation of the fluvial scarp, the slope above it became destabilized, which initiated the down-slope transport of sediment. Between January 20, 2011, and May 12, 2011, the slope above the fluvial scarp eroded about 0.7 m (fig. 12B). This erosion undermined the crest of the cutbank and formed a near-vertical free face (fig. 12A). From May 2011 to February 2013, the top of the fluvial scarp and upper part of the cutbank continued to erode and shed sediment down slope. Horizontal erosion of greater than 0.5 m at the upper part of the cutbank caused the free face to further enlarge (figs. 12A, C). The simultaneous down-slope transport of colluvium accumulated horizontally up to 1.0 m on the lower part of the cutbank (figs. 12A, C). The erosion on the upper half of the cutbank and deposition below returned the slope angle to a value at, or near, the angle of repose (fig. 12A). For the 4-m-wide swath shown in figure 12, the net horizontal change (bank retreat) from January 2011 to February 2013 was generally on the order of 0.9 plus or minus 0.3 m (fig. 12D). A notable exception to this was near the top of the cutbank, where the net effect of the bank retreat was a steepening of the slope angle and horizontal erosion of about 0.3 m (figs. 12A, D).

Summary

The purpose of this report is to document the methods used to quantify the volume of mercury (Hg)-contaminated sediment eroded from a discrete section of stream cutbank along Deer Creek at Stocking Flat, an area which is managed by the Bureau of Land Management (BLM), and to report the eroded volume results for three periods between December 1, 2010, and February 4, 2013 (incremental and total volume). The sequential terrestrial laser scanning (TLS) data also provide information regarding the physical processes of cutbank erosion. This latter information could be useful to the BLM for the purpose of the stabilizing of Hg-contaminated sediment at Stocking Flat and similar sites elsewhere. A suite of innovative visualization graphics, including two-dimensional (2-D) maps and three-dimensional (3-D) images, are also included.

Sequential TLS has proven to be an effective tool to quantify volumetric changes of a complex, eroding surface that could not have been mapped non-destructively or in sufficient detail using traditional surveying techniques. The non-destructive scanning of the unconsolidated cutbank sediments and the sub-centimeter precision of the resulting point clouds allowed for a spatially detailed assessment of change across the cutbank surface. In this study, four sequential TLS surveys of the stream cutbank were carried out. Each survey was composed of multiple TLS scans collected from different vantage points, which were combined into a composite 3-D point cloud of the stream cutbank. The sequential surveys were co-registered, or ‘aligned,’ into a common 3-D reference frame so that volumetric comparisons between the surveys could be made. The utilization of virtual-reality technology to inspect the alignment of the light detection and ranging (lidar) point-cloud data enabled the isolation of features more intuitively, quickly, and accurately than previously possible with non-immersive 2-D environments and greatly improved the level of confidence in data quality prior to analysis. The differences between sequential surveys indicated the amount (volume) of sediment removed from the cutbank by erosion.

From December 1, 2010, to January 20, 2011, a minimum of 143 plus or minus 15 cubic meters (m³) of Hg-contaminated sediment was eroded from the Stocking Flat cutbank study site. From January 20, 2011, to May 12, 2011, an additional 207 plus or minus 24 m³ or more of sediment was eroded from the cutbank. Combining these two measurements, the total minimum volume of Hg-contaminated sediment eroded by Deer Creek during the period from December 1, 2010, through May 12, 2011, was 350 plus or minus 28 m³. From May 12, 2011, to February 4, 2013, an additional 18 plus or minus 10 m³ or more of Hg-contaminated sediment was eroded. The total volume of eroded sediment from December 1, 2010, through February 4, 2013, was at least 368 plus or minus 30 m³ (table 2).

The analysis of sequential TLS data by using 2-D visualization techniques, such as oblique-perspective, shaded-relief imagery, and color-coded change maps, as well as stereoscopic 3-D anaglyphs, can enhance the understanding of complex 3-D data sets, aid with the interpretation of physical processes, and help with the design of remediation and mitigation measures.

The results of this study are to be used in combination with laboratory data for Hg concentration and grain-size distribution (Jacob Fleck and others, U.S. Geological Survey, written commun., 2015) to quantify the amount of Hg eroded into Deer Creek during this period. Results from these investigations are for use by the BLM, in consultation with other federal, state, and local agencies, as well as other interested parties, to determine whether removal or stabilization of Hg-contaminated sediment is needed at the Stocking Flat site. These results can be used by the BLM to prioritize future remediation activities related to abandoned mines and mine wastes in the Deer Creek drainage basin.

References Cited

- Alpers, C.N., Hunerlach, M.P., May, J.T., and Hothem, R.L., 2005a, Mercury contamination from historical gold mining in California: U.S. Geological Survey Fact Sheet 2005–3014, 6 p., available at <http://pubs.usgs.gov/fs/2005/3014/>.
- Alpers, C.N., Hunerlach, M.P., May, J.T., Hothem, R.L., Taylor, H.E., Antweiler, R.C., De Wild, J.F., and Lawler, D.A., 2005b, Geochemical characterization of water, sediment, and biota affected by mercury contamination and acidic drainage from historical gold mining, Greenhorn Creek, Nevada County, California, 1999–2001: U.S. Geological Survey Scientific Investigations Report 2004–5251, 278 p., available at <http://pubs.usgs.gov/sir/2004/5251/>.
- Alpers, C.N., Hunerlach, M.P., Marvin-DiPasquale, M.C., Antweiler, R.C., Lasorsa, B.K., De Wild, J.F., and Snyder, N.P., 2006, Geochemical data for mercury, methylmercury, and other constituents in sediments from Englebright Lake, California, 2002: U.S. Geological Survey Data Series 151, 95 p., available at <http://pubs.usgs.gov/ds/2006/151/>.
- Alpers, C.N., Fleck, J.A., Beaulieu, Elizabeth, Hothem, R.L., May, J.T., Marvin-DiPasquale, M.C., Blum, A.E., and Graves, P.G., 2012, Characterization of mercury and methylmercury contamination in stream and pond environments and provenance of mine waste from historical gold mining in the Sierra Nevada, California [abs.]: U.S. Environmental Protection Agency Hard-rock Mining Conference, April 3–5, 2012, Denver, Colorado, Advancing solutions for a new legacy, p. 103–104, available at https://clu-in.org/download/issues/mining/Hard_Rock_ConferenceHandout/HRM_2012_Handout.pdf.
- Churchill, R.K., 2000, Contributions of mercury to California’s environment from mercury and gold mining activities: Insights from the historical record, *in* Extended abstracts for the U.S. Environmental Protection Agency sponsored meeting, Assessing and Managing Mercury from Historic and Current Mining Activities, November 28–30, 2000, San Francisco, Calif., EPA/325/R-04/102; p. 33–36 and S35–S48, available at https://cfpub.epa.gov/si/si_public_record_Report.cfm?dirEntryId=96732&CFID=15005568&CFTOKEN=17523643.
- Fleck, J.A., Alpers, C.N., Marvin-DiPasquale, M.C., Hothem, R.L., Wright, S.A., Ellett, Kevin, Beaulieu, Elizabeth., Agee, J.L., Kakouros, Evangelos, Kieu, L.H., Eberl, D.D., Blum, A.E., and May, J.T., 2011, The effects of sediment and mercury mobilization in the South Yuba River and Humbug Creek confluence area, Nevada County, California: Concentrations, speciation, and environmental fate—Part 1: Field characterization: U.S. Geological Survey Open-File Report 2010–1325A, 104 p., available at <http://pubs.usgs.gov/of/2010/1325A>.

22 Quantifying Mercury-Contaminated Sediment at Stocking Flat, Deer Creek, Nevada County, Calif., 2010–13

- Gilbert, G.K., 1917, Hydraulic-mining debris in the Sierra Nevada: U.S. Geological Survey Professional Paper 105, 154 p., available at: <https://pubs.er.usgs.gov/publication/pp105>.
- Heritage, G.L. and Large, A.R.G., 2009, Laser scanning for the environmental sciences, Wiley-Blackwell Publishing, ISBN 978-1-4051-5717-9, 278 p.
- Hunerlach, M.P., Rytuba, J.J., and Alpers, C.N., 1999, Mercury contamination from hydraulic placer-gold mining in the Dutch Flat mining district, California, *in* Morganwalp, D.W., and Buxton, H.T. (eds.), U.S. Geological Survey Toxic Substances Hydrology Program – Proceedings of the Technical Meeting, Charleston, South Carolina, March 8–12, 1999, U.S. Geological Survey Water-Resources Investigations Report 99–4018B, p. 179–189, available at <http://ca.water.usgs.gov/mercury/dutch/wrir994018b.pdf>.
- Hunerlach, M.P., Alpers, C.N., Marvin-DiPasquale, M.C., Taylor, H.E., and De Wild, J.F., 2004, Geochemistry of mercury and other trace elements in fluvial tailings upstream of Daguerre Point Dam, Yuba River, California: U.S. Geological Survey Scientific Investigations Report 2004–5165, 66 p., available at <http://pubs.usgs.gov/sir/2004/5165/>.
- James, L.A., 1989, Sustained storage and transport of hydraulic mining sediment in the Bear River, California: *Annals Association of American Geographers*, v. 79, no. 4, p. 570–592.
- Kellogg, L.H., Bawden, G.W., Bernardin, Tony, Billen, Magali, Cowgill, Eric, Hamann, Bernd, Jadamec, Margarete, Kreylos, Oliver, Staadt, Oliver, and Sumner, Dawn, 2008, Interactive visualization to advance earthquake simulation: *Pure and Applied Geophysics*, v. 165, no. 3, p. 621–633. DOI 10.1007/s00024-008-0317-9.
- Kreylos, Oliver, Bawden, G.W., and Kellogg, L.H., 2008, Immersive visualization and analysis of LiDAR data, *in* Bebis, G., and others, *Advances in Visual Computing, Proceedings Part I, 4th International Symposium on Visual Computing, December 1–3, 2008, Las Vegas, Nevada: Lecture Notes in Computer Science*, v. 5358, p. 846–855, available at <http://link.springer.com/book/10.1007/978-3-540-89639-5/page/5>.
- Marvin-DiPasquale, Mark, Agee, J.L., Kakouros, Evangelos, Kieu, L.H., Fleck, J.A., and Alpers, C.N., 2011, The effects of sediment and mercury mobilization in the South Yuba River and Humbug Creek confluence area, Nevada County, California: Concentrations, speciation and environmental fate—Part 2: Laboratory Experiments: U.S. Geological Survey, Open-File Report 2010–1325B, 53 p., available at <http://pubs.usgs.gov/of/2010/1325B>.
- May, J.T., Hothem, R.L., Alpers, C.N., and Law, M.A., 2000, Mercury bioaccumulation in fish in a region affected by historic gold mining: The South Yuba River, Deer Creek, and Bear River watersheds, California, 1999: U.S. Geological Survey Open-File Report 00–367, 30 p., available at <http://ca.water.usgs.gov/archive/reports/ofr00367/index.html>.
- Tufte, E.R., 1983, *The visual display of quantitative information*, second edition: Cheshire, Connecticut, Graphics Press, 193 p.

Glossary

Anaglyph image: A stereoscopic three-dimensional (3-D) effect achieved by encoding images with chromatically different colors (typically red and blue) for each eye. When viewed through the color-coded anaglyph glasses (red and blue lens glasses), each of the images reaches one eye, giving the depth perception of a 3-D scene.

Angle of repose: The maximum angle, relative to the horizontal plane, at which sediment of a given particle size and degree of rounding will remain stable without sliding down slope.

Colluvium: A general term for loose, unconsolidated sediments that have been eroded from a higher slope position (typically a steeper slope) and deposited down slope (typically on a lower angle slope) by gravity-driven processes.

Dry ravel: A general term that describes the gravity-driven rolling, bouncing, and sliding of sediment particles down a slope.

Hard-rock mining: A general term that refers to various methods used to excavate hard minerals, typically those containing precious and base metals such as gold, silver, copper, zinc, and lead. In the Sierra Nevada of California, hard-rock mining of low-sulfide gold-quartz vein deposits was primarily done by underground methods.

Hydraulic gold mine: A type of surface mine where a high-pressure jet of water (emitted from a water cannon, or monitor) is used to dislodge or erode gold-bearing sedimentary deposits exposed on a hillside or cliff face. The practice was largely banned in California starting in 1884.

Kriging: A weighted statistical technique used to interpolate a value based on the spatial covariance of surrounding data points. In this study, the kriged or interpolated values are points on the surface of the cutbank between existing lidar data points.

Lidar: Light detection and ranging is a remote-sensing technology used to make precise three-dimensional “point clouds” of the land surface. Sometimes lidar is referred to as terrestrial laser scanning (TLS). Pulses of near-infrared laser light are timed to measure the distance (range) from the lidar scanner to the reflecting surface. Laser ranges are combined with angular orientation data to generate a dense and detailed set of points (locations of individual laser returns) referred to as a point cloud.

Mining debris: Waste materials from mining (including hydraulic mining) and mineral processing, including waste rock and mill tailings from hard-rock mines. Waste rock is material below ore grade that is separated from economically viable ore. Waste rock typically is not milled, so it consists of material including large clasts or cobbles. Mill tailings are what remain after the milling process has separated out the valuable fraction of an ore, leaving waste material that is typically sand-sized or smaller particles.

Placer mining: Mining of an unconsolidated alluvial or colluvial deposit (placer deposit). Typically, placer deposits are mined by surface methods (hydraulic mining or dredging); in some cases, underground methods (drift mining) are used. Metallic clasts and mineral grains are gravity separated by means of hydraulic saturation, mechanical agitation, or both.

Point cloud: A point cloud is a set of vertices in a three-dimensional coordinate system. These vertices are usually defined by x, y, and z coordinates and typically represent the external surface of an object.

Terrestrial laser scanning (TLS): Sometimes referred to as terrestrial lidar or tripod-mounted lidar (T-lidar). ‘Terrestrial’ refers to the laser scanner being used near the Earth’s surface (stationary on a tripod) as opposed to airborne laser scanning (ALS).

Water year: A 12-month period, offset from the calendar year, that brackets seasonal precipitation typically associated with the winter and spring months. The U.S. Geological Survey water year (WY) starts on October 1 and ends on September 30 of the following year; for example, WY 2011 started October 1, 2010, and ended September 30, 2011.

Red-blue glasses (with the red lens on the right side) are needed for enhanced 3-D viewing of the following figures in this report: 11A, 11C, 11E, 11G, and 12A. To request red-blue glasses, please contact James Howle by phone (530-587-0910, ext. 2017) or by email (jfhowle@usgs.gov).

Prepared by the Sacramento Publishing Service Center.

For more information concerning this report, contact:

Director
U.S. Geological Survey
California Water Science Center
6000 J Street, Placer Hall
Sacramento, CA 95819
dc_ca@usgs.gov

or visit our Web site at:
<http://ca.water.usgs.gov>

